Le Friant, A.; Ishizuka, O.; Boudon, G.; Palmer, M.R.; **Talling, P.J.**; Villemant, B.; Adachi, T.; Aljahdali, M.; Breitkreuz, C.; Brunet, M.; Caron, B.; Coussens, M.; Deplus, C.; Endo, D.; Feuillet, N.; Fraas, A.J.; Fujinawa, A.; Hart, M.B.; Hatfield, R.G.; Hornbach, M.; **Jutzeler, M.**; Kataoka, K. S.; Komorowski, J-C.; Lebas, E.; Lafuerza, S.; Maeno, F.; Manga, M.; Martínez-Colón, M.; McCanta, M.; Morgan, S.; Saito, T.; Slagle, A.; Sparks, S.; Stinton, A.; Stroncik, N.; Subramanyam, K.S.V.; Tamura, Y.; Trofimovs, J.; Voight, B.; Wall-Palmer, D.; Wang, F.; Watt, S.F.L.. 2015
Submarine record of volcanic island construction and collapse in the Lesser Antilles arc: First scientific drilling of submarine volcanic island landslides by IODP Expedition 340. *Geochemistry, Geophysics, Geosystems*, 16 (2). 420-442.
10.1002/2014GC005652

AGU PUBLICATIONS

Geochemistry, Geophysics, Geosystems

RESEARCH ARTICLE

10.1002/2014GC005652

Key Points:

- First drilling of large and likely tsunamigenic volcanic island-arc landslides
- Distal landslide deposits recovered seafloor sediment (turbidite, hemipelagic)
- Debris avalanche emplacement can trigger voluminous seafloor sediment failure

Correspondence to:
A. Le Friant,
lefriant@ipgp.fr

Citation:
Friant, A., et al. (2015), Submarine record of volcanic island construction and collapse in the Lesser Antilles arc: First scientific drilling of submarine volcanic island landslides by IODP Expedition 340, *Geochem. Geophys. Geosyst.*, *16*, 420–442, doi:10.1002/2014GC005652.

Received 6 NOV 2014
Accepted 24 DEC 2014
Accepted article online 6 JAN 2015
Published online 11 FEB 2015

Submarine record of volcanic island construction and collapse in the Lesser Antilles arc: First scientific drilling of submarine volcanic island landslides by IODP Expedition 340

A. Le Friant[1], O. Ishizuka[2], G. Boudon[1], M. R. Palmer[3], P. J. Talling[4], B. Villemant[5], T. Adachi[6], M. Aljahdali[7], C. Breitkreuz[8], M. Brunet[1], B. Caron[5], M. Coussens[4], C. Deplus[1], D. Endo[9], N. Feuillet[1], A. J. Fraas[10], A. Fujinawa[11], M. B. Hart[12], R. G. Hatfield[13], M. Hornbach[14], M. Jutzeler[4], K. S. Kataoka[15], J.-C. Komorowski[1], E. Lebas[1,16], S. Lafuerza[1,17], F. Maeno[18], M. Manga[19], M. Martínez-Colón[20], M. McCanta[21], S. Morgan[22], T. Saito[23], A. Slagle[24], S. Sparks[25], A. Stinton[26], N. Stroncik[27], K. S. V. Subramanyam[28], Y. Tamura[29], J. Trofimovs[30], B. Voight[31], D. Wall-Palmer[32], F. Wang[33], and S. F. L. Watt[34]

[1]Institut de Physique du Globe de Paris, Sorbonne Paris Cite, Universite Paris Diderot, CNRS UMR 7154, 1, rue Jussieu, Paris, France, [2]Geological Survey of Japan, AIST, Tsukuba, Japan, [3]School of Ocean and Earth Science, University of Southampton, Southampton, UK, [4]National Oceanography Center, University of Southampton, Southampton, UK, [5]Laboratoire de Petrologie, Geochimie, Volcanologie, University Pierre et Marie Curie-Paris 6, UMR 7193, ISTEP, Paris, France, [6]Graduate School of Science and Engineering, Yamagata University, Kojirakawa-machi, Japan, [7]Department of Earth, Ocean, and Atmospheric Sciences, Florida State University, Tallahassee, Florida, USA, [8]Department of Geology and Paleontology, TU Bergakademie Freiberg, Freiberg, Germany, [9]A203, Earth Evolution Sciences, University of Tsukuba, Tsukuba, Japan, [10]Department of Geosciences, University of Massachusetts Amherst, Amherst, Massachusetts, USA, [11]Department of Environmental Sciences, Ibaraki University, Mito, Japan, [12]Centre for Research in Earth Sciences, Plymouth University, Plymouth, UK, [13]CEOAS, Oregon State University, Corvallis, Oregon, USA, [14]Department of Earth Sciences, Southern Methodist University, Dallas, Texas, USA, [15]Research Institute for Natural Hazards and Disaster Recovery, Niigata University, Niigata, Japan, [16]Now at Geomar Helmholtz Centre for Ocean Research, Kiel, Germany, [17]Now at Fugro GeoConsulting SAS, 39 rue des Peupliers, Nanterre, France, [18]Volcano Research Center, Earthquake Research Institute, University of Tokyo, Tokyo, Japan, [19]Department of Earth and Planetary Science, University of California, Berkeley, California, USA, [20]College of Marine Science, University of South Florida, St. Petersburg, Florida, USA, [21]Geology Department, Tufts University, Medford, Massachusetts, USA, [22]Department of Geology, University of Leicester, Leicester, UK, [23]International Researchers Empowerment Center, Shinshu University, Matsumoto, Japan, [24]Borehole Research Group, Lamont-Doherty Earth Observatory, Earth Institute at Columbia University, Palisades, New York, USA, [25]School of Earth Sciences, University of Bristol, Bristol, UK, [26]Montserrat Volcano Observatory, Flemmings, Montserrat, West Indies, [27]Institut für Erd- Und Umweltwissenschaften, Universität Potsdam, Potsdam, Germany, [28]Geochemistry Division, National Geophysical Research Institute, Hyderabad, Telangana, India, [29]Institute for Research on Earth Evolution, JAMSTEC, Yokosuka, Japan, [30]Queensland University of Technology, Brisbane, Australia, [31]Department of Geosciences, Penn State University, University Park, Pennsylvania, USA, [32]School of Geography, Earth, and Environmental Sciences, Plymouth University, Plymouth, UK, [33]Institute of Geology and Geophysics, Chinese Academy of Sciences, Beijing, China, [34]School of Geography, Earth, and Environmental Sciences, University of Birmingham, Birmingham, UK

Abstract IODP Expedition 340 successfully drilled a series of sites offshore Montserrat, Martinique and Dominica in the Lesser Antilles from March to April 2012. These are among the few drill sites gathered around volcanic islands, and the first scientific drilling of large and likely tsunamigenic volcanic island-arc landslide deposits. These cores provide evidence and tests of previous hypotheses for the composition and origin of those deposits. Sites U1394, U1399, and U1400 that penetrated landslide deposits recovered exclusively seafloor sediment, comprising mainly turbidites and hemipelagic deposits, and lacked debris avalanche deposits. This supports the concepts that i/ volcanic debris avalanches tend to stop at the slope break, and ii/ widespread and voluminous failures of preexisting low-gradient seafloor sediment can be triggered by initial emplacement of material from the volcano. Offshore Martinique (U1399 and 1400), the landslide deposits comprised blocks of parallel strata that were tilted or microfaulted, sometimes separated by intervals of homogenized sediment (intense shearing), while Site U1394 offshore Montserrat penetrated a flat-lying block of intact strata. The most likely mechanism for generating these large-scale seafloor sediment failures appears to be propagation of a decollement from proximal areas loaded and incised by a volcanic debris avalanche. These results have implications for the magnitude of tsunami generation. Under some conditions, volcanic island landslide deposits composed of mainly seafloor sediment will tend to form

smaller magnitude tsunamis than equivalent volumes of subaerial block-rich mass flows rapidly entering water. Expedition 340 also successfully drilled sites to access the undisturbed record of eruption fallout layers intercalated with marine sediment which provide an outstanding high-resolution data set to analyze eruption and landslides cycles, improve understanding of magmatic evolution as well as offshore sedimentation processes.

1. Introduction

Volcano flank-collapses include the largest volume landslides on our planet [*Masson et al*., 2006] and are increasingly recognized as a common and important process in the construction and destruction of volcanic edifices [*Glicken*, 1986; *Ida and Voight*, 1995; *McGuire*, 1996; *Voight*, 2000]. The most voluminous events occur on volcanic islands, such as Hawaii [*Lipman et al*., 1988; *Moore et al*., 1989], La Réunion [*Labazuy*, 1996; *Oehler et al*., 2008; *Le Friant et al*., 2011] and in the Canary Archipelago [*Holcomb and Searle*, 1991; *Watts and Masson*, 1995; *Urgeles et al*., 1997; *Krastel et al*., 2001; *Masson et al*., 2002, 2006], where individual landslide deposits can contain hundreds to thousands of cubic kilometers of material. The recognition of flank-collapse events is commonly based on mapping subaerial horseshoe-shaped structures, which can often be traced to on-shore and/or offshore landslide deposits [*Voight et al*., 1981]. Offshore deposits typically display hummocky morphology on bathymetry and/or chaotic facies on seismic reflection profiles [*Deplus et al*., 2001; *Le Friant et al*., 2002, 2003a, 2004, 2008; *Lebas et al*., 2011; *Watt et al*., 2012a, 2012b]. Volcano collapse events play a significant role in the evolution of volcanic edifices, affecting the dynamics of subsequent eruptions [*Pinel and Albino*, 2013] and the process dynamics in shallow magma reservoirs [*Pinel and Jaupart*, 2000; *Boudon et al*., 2013].

Volcano flank-collapses are a significant component of volcanic hazards that also include associated explosive eruptions and tsunamis. Understanding how flank collapses are emplaced is important because collapse dynamics determine the magnitude of associated tsunamis. The potential magnitude of tsunamis generated by volcanic island collapses is the subject of vigorous debate, mainly due to uncertainty on how collapsed material enters the ocean [*Slingerland and Voight*, 1979; *Ward and Day*, 2001; *Masson et al*., 2006; *Mattioli et al*., 2007; *Løvholt et al*., 2008; *Hunt et al*., 2011; *Watt et al*., 2012a, 2012b, 2014].

Here we report on the first scientific drilling of volcanic-arc island landslide deposits by IODP Expedition 340, offshore Montserrat, Martinique and Dominica in the Lesser Antilles arc (Figure 1). Areas of intraplate active volcanism have previously been drilled by the Ocean Drilling Program such as in Hawaii (ODP legs 126 and 200) [*Garcia*, 1993, *Garcia et al*., 1994, 2006] or around the Canary Islands (ODP leg 157) [*Schneider et al*., 1997, *Goldstrand*, 1998, *Schmincke and Sumita*, 1998]. These previous ODP drill sites mainly targeted distal turbidite deposits away from seismically chaotic landslide deposits recognized in more proximal settings, although Leg 157 drilled turbidite deposits in proximal parts of the island edifice.

1.1. Interest of the Lesser Antilles Arc and Previous Data

The Lesser Antilles island arc results from subduction of Atlantic oceanic crust beneath the Caribbean plate (Figure 1). Recent convergence of the plates has been slow ($\sim$ 2 cm yr^{-1}) [*Feuillet et al*., 2002] and magma productivity has been low relative to other arcs, estimated at 3–5 km^3 Ma^{-1} km^{-1}; [*Sigurdsson et al*., 1980; *Wadge*, 1984; *MacDonald et al*., 2000]. Arc volcanism has been active since 40 Ma [*Martin-Kaye*, 1969; *Bouysse et al*., 1990]. North of Dominica, the arc is divided into two chains of islands and built on a Cretaceous ocean island arc [*Bouysse and Guennoc*, 1983; *Wadge*, 1986]. The eastern chain corresponds to an older extinct arc (Eocene to early Miocene) where thick carbonate platforms now cover the volcanic basement while the western chain is the site of active volcanism. South of Dominica, the older and recent arcs are superimposed, forming a chain of islands bordered to the west by the 2900 m deep back-arc Grenada Basin. This basin has been a major depocentre for large mass-wasting deposits, volcanogenic turbiditic deposits, pyroclastic flow deposits, and hemipelagic sediment [*Sigurdsson et al*., 1980; *Deplus et al*., 2001; *Picard et al*., 2006; *Boudon et al*., 2007] (Figures 1 and 2).

The Lesser Antilles volcanic arc is well suited to study of volcanic island growth and collapse. Since the mid-Oligocene, volcanic activity has constructed numerous volcanic edifices. At least 12 of these edifices have

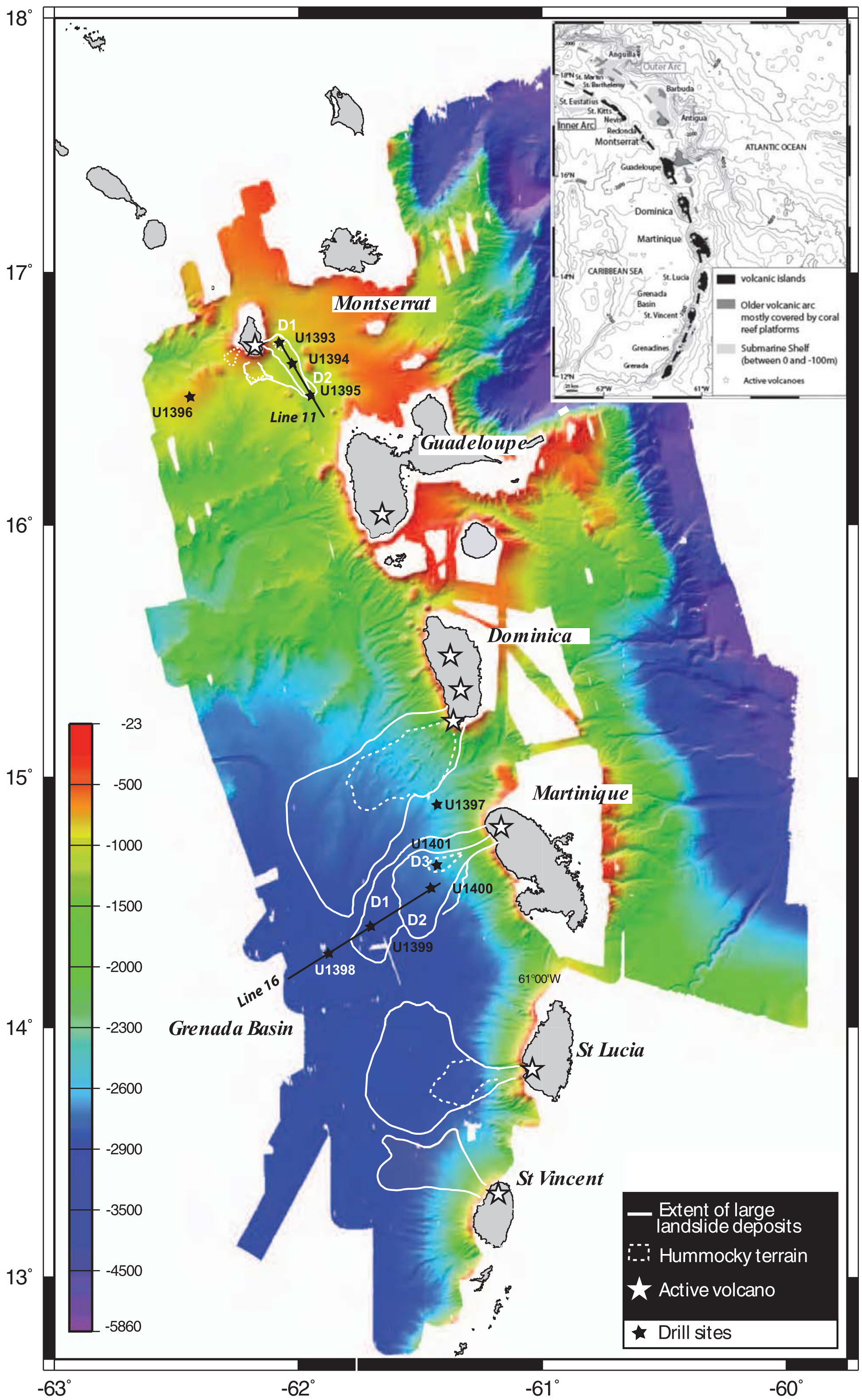

Figure 1. The Lesser Antilles arc. Extent of chaotic units on swath bathymetry illuminated from the North (Aguadomar cruise, 1999 and Caraval cruise, 2002, IPGP-INSU). Active volcanoes and drilling sites are annotated. Solid lines represent the seismic profiles shown in Figure 4.

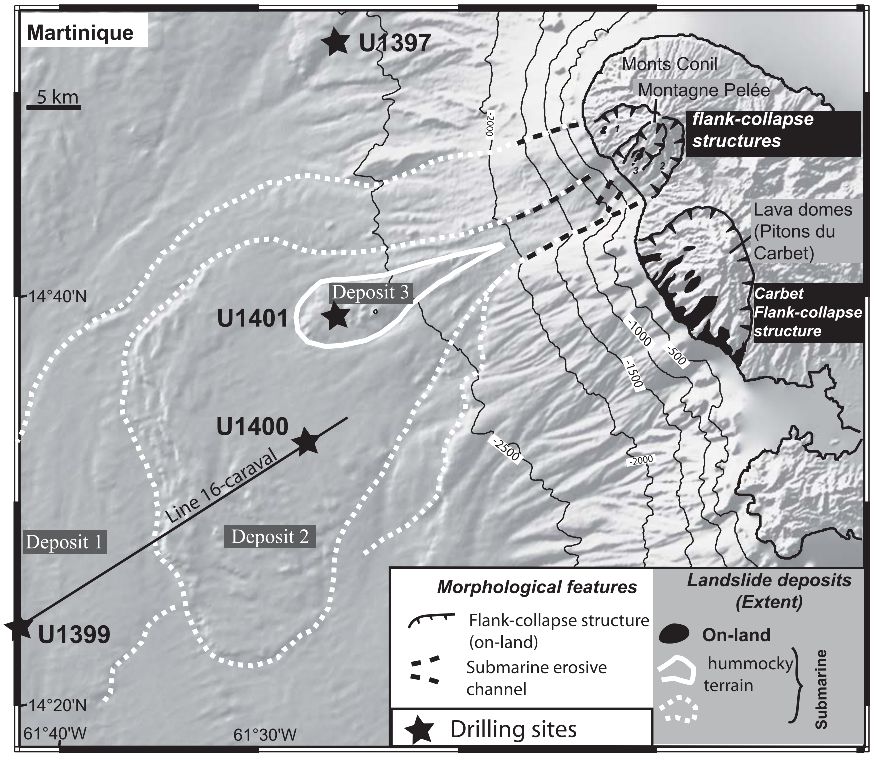

Figure 2. Shaded image of combined bathymetry and topography data of Martinique Island and submarine slopes. Marine landslide deposits and on-land flank-collapse structures are outlined. Drilling sites are annotated as well as location of seismic profiles.

been active in the last 10,000 years, and they are characterized by an exceptional diversity of arc magma compositions and eruptive styles, with marked differences along the arc from north to south [*MacDonald et al*., 2000].

The most complete record of major volcanic activity and landslides is typically found offshore from volcanic islands rather than in onshore deposits, as terrestrial deposits may be removed by erosion or buried by subsequent volcanic activity. Further, many large landslides are energetic enough to move completely into the ocean, leaving little to no depositional evidence onshore. In the Lesser Antilles, *Le Friant et al*. [2009, 2010] showed that up to 70% by volume of the erupted products from the 1995-recent eruption of Soufrière Hills volcano on Montserrat were deposited directly into the surrounding ocean, or rapidly eroded and transported to the ocean shortly after temporary deposition on land (Figures 1 and 3). Marine deposits are also more often easily dated using layers of intervening hemipelagic mud, making marine sediments an important repository of volcanic arc history [*Paterne*, 1985, *Paterne et al*., 2008; *Le Friant et al*., 2008; *Trofimovs et al*., 2013, *Boudon et al*., 2013]. Seismic data are also more easily collected offshore than on rugged terrestrial edifices, and very detailed seismic data are available offshore Montserrat and Martinique, including dense 2-D and 3-D data sets. These seismic data provide high-resolution images of the extent, internal character and basal contact of landslide deposits (Figure 4) [*Deplus et al*., 2001; *Le Friant et al*., 2003a, 2008; *Lebas et al*., 2011; *Watt et al*., 2012a, 2012b; *Crutchley et al*., 2013; *Karstens et al*., 2013], and such information can be combined with detailed bathymetric mapping of the surface expression of the most recent landslides. Offshore Montserrat, a closely spaced set of shallow (< 6 m long) piston cores also provides a detailed chronology of events during the last ~130 ka [*Trofimovs et al*., 2006, 2008, 2010, 2012, 2013; *Cassidy et al*., 2013], supplementing data from terrestrial outcrops [e.g., *Harford et al*., 2002; *Druitt and Kokelaar*, 2002; *Sparks et al*., 2002, *Lindsay et al*., 2005; *Smith et al*., 2007].

At least 52 individual landslides have been identified on the flanks of volcanoes of the Lesser Antilles arc (Figures 1–3) [e.g., *Boudon et al*., 1984, 1987, 2007; *Vincent et al*., 1989; *Deplus et al*., 2001; *Le Friant et al*., 2002, 2003a, 2003b, 2004; *Komorowski et al*., 2005; *Lebas et al*., 2011; *Watt et al*., 2012a, 2012b; *Crutchley et al*., 2013; *Karstens et al*., 2013; *Trofimovs et al*., 2006, 2010, 2013; *Cassidy et al*., 2014]. Past analysis of seismic profiling data offshore Montserrat and Martinique has resulted in a series of hypotheses concerning the

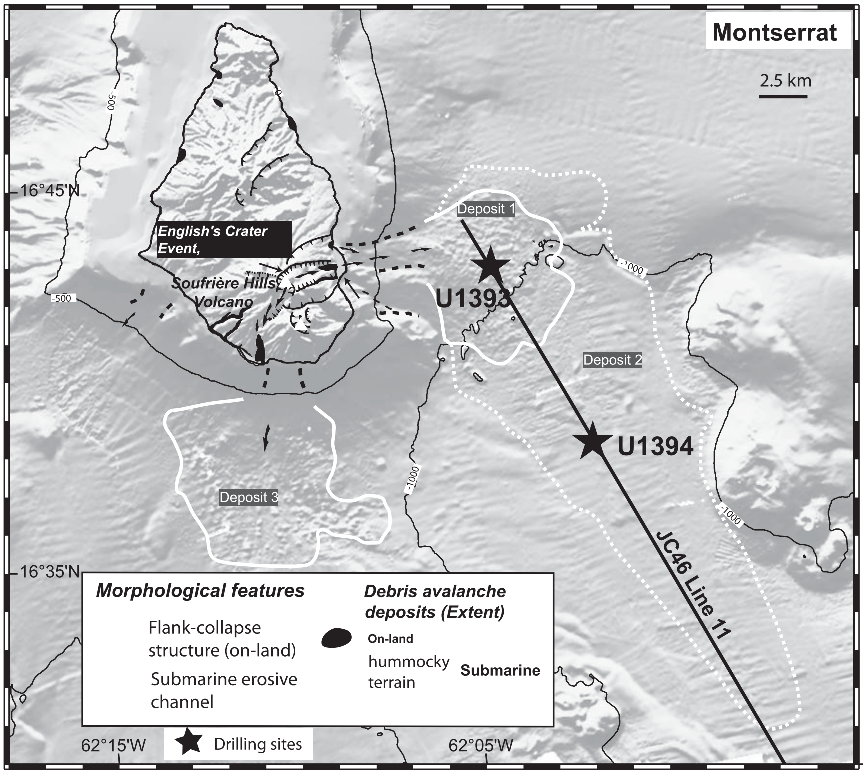

Figure 3. Montserrat and the surrounding seafloor showing marine landslide deposits outlines. Location of drilling sites is annotated as well as location of the seismic profile from **Figure**. 4.

composition of submarine landslide deposits. Using seismic profile data *Deplus et al*. [2001] and *Le Friant et al*. [2002, 2003a, 2003b, 2004] mapped numerous landslide deposits along the arc. They proposed, based on these data, that debris avalanches erode and mobilize preexisting layers of seafloor sediment, and thus disturb underlying layers of preexisting sediment. They suggested that the upper part of the seismically chaotic landslide deposit thus comprises both volcanic debris from the original edifice collapse and remobilized preexisting seafloor sediment, while the lower part mainly comprises deformed preexisting seafloor sediment. Lateral transitions from well-bedded seafloor sediment into chaotic landslide deposits indicate that some landslides internally contain a substantial component of seafloor-derived sediment (Figure 4). *Deplus et al*. [2001] also emphasize that a substantial amount of material derived from the submarine part of the volcanic edifice is commonly involved in generation of the deposits, as shown by chutes cut into the volcano flanks. *Le Friant et al*. [2004] integrated this information to outline how terrestrial collapse scars, submarine chutes and offshore debris avalanche deposits were linked to the geomorphological evolution of Montserrat. *Le Friant et al*. [2004] and *Lebas et al*. [2011] also used seismic data to accurately define the extent and volume of the landslide deposits offshore Montserrat, and demonstrated that the volumes of submarine landslide deposits may be much greater than the volume of the associated subaerial collapse scars, requiring that landslide events may include a significant fraction from the volcano's submerged flank or adjacent seafloor sediment. Truncation of in situ bedded sediment packages was attributed to erosional processes during debris avalanche emplacement. *Lebas et al*. [2011] also proposed that strong seismic reflectors seen at the base of some landslide deposits may be produced by slide-derived shear zones. *Watt et al*. [2012a, 2012b, 2014] also proposed that emplacement of material from the volcanic edifice (i.e., a volcanic debris avalanche) caused erosion and triggered failure of seafloor sediment. Such seafloor sediment failure could be very widespread on low ($< 1^\circ$) gradients, and may dominate the total landslide volume. Their data are consistent with the concept that rapid emplacement of the volcanic edifice material onto the seafloor led to undrained shear loading and failure of underlying seafloor sediment layers [*Voight and Elsworth*, 1997; *Voight et al*., 2012]. A wave of such deformation then propagated long distances downslope through the seafloor sediment into areas of seafloor which otherwise were not on the verge of failure [*Viesca and Rice*, 2012]. *Watt et al*. [2012a, 2012b] further noted a lack of frontal compression and shear

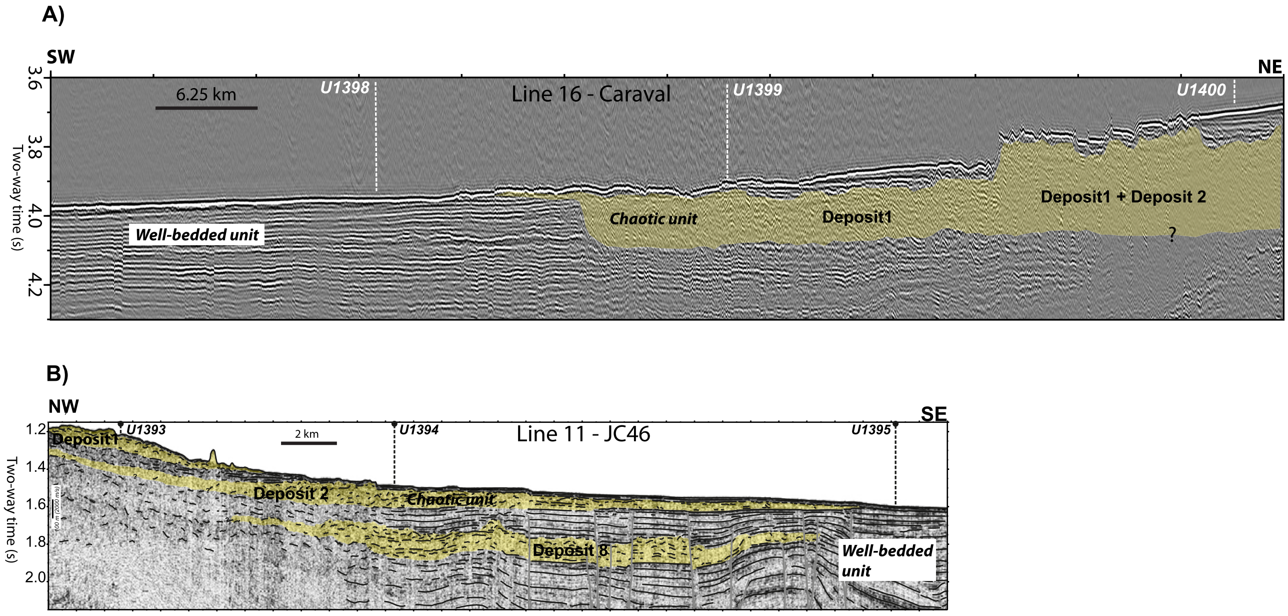

Figure 4. Seismic reflection profiles revealing the presence of chaotic deposits offshore Martinique and Montserrat. Location of profiles is shown on Figures 1 and 3. Deposits are characterized by chaotic reflectors that contrast with well-bedded subhorizontal sedimentary units. The locations of drilling sites are annotated. (a) Caraval, Line 16 offshore Martinique. (b) JC45, Line 11 offshore Montserrat.

breakout [e.g., *Frey-Martinez et al*., 2006], suggesting that much of the deformed seafloor material they observed did not move for extensive distances. They also proposed that some landslide deposits may have incorporated large blocks of relatively undeformed seafloor sediment. Finally, the amount, nature, velocity and location of failure of seafloor sediment affect the process and scale of tsunami generation. Landsides occurring in deep (>500 m) seafloor sediment tend to form smaller magnitude tsunamis since the Froude number is too low to generate a significant wave [*Ward*, 2001]. Overall, slow failures of deep seafloor sediment cause much smaller tsunamis than debris avalanches derived from the volcanic edifice, even if the seafloor sediment failure has a much greater volume [*Watt et al*., 2012a; *Ward*, 2001].

1.2. Objectives of This Contribution

IODP Expedition 340 drilled a series of sites offshore Montserrat, Martinique and Dominica in the Lesser Antilles from March to April 2012. These comprise some of the few drill sites around volcanic islands, and represent the first scientific drilling of volcanic island-arc landslide deposits. Here we discuss the initial key results from Expedition 340, and address the following specific questions:

1. What is the composition of voluminous chaotic units identified on seismic profiles associated with the volcanic island landslides? In particular, what is the relative contribution of material derived from the subaerial or submarine volcanic edifice, versus material originating from failure of preexisting seafloor sediment? Can we thus explain the observed discrepancy between the constrained size of the on-land flank-collapse structures, and the much larger volume of associated submarine landslide deposits [*Le Friant et al*., 2003a; *Boudon et al*., 2007; *Lebas et al*., 2011]?

2. What types of deformation are seen within the cored volcanic island landslide deposits? What can we learn about their emplacement? What are the mechanisms of the landslide generation and propagation? How do these new field observations relate to predictions made by previously proposed models [*Voight and Elsworth*, 1997; *Deplus et al*., 2001; *Le Friant et al*., 2004; *Lebas et al*., 2011, *Watt et al*., 2012a, 2012b, 2014; *Voight et al*., 2012].

3. More generally, what is the importance of mass-wasting events for sedimentation around volcanic islands, and what processes affect the sedimentation in such settings? What are the ages of these events and how do they relate to the eruptive history of Lesser Antilles volcanoes (including timing, eruptive style,

chronology, magma composition and production rates)? How can we use this information for assessing the geohazard potential of such systems?

1.3. Terminology

We propose a clearly defined and consistent terminology before presenting the initial results of Expedition 340. *Landslide* is used as a general term for any type of slope failure and resulting mass movement, whether initiating onshore or offshore. The term *debris avalanche* is used for a failure comprising material in a mobile flowage-type landslide from a volcanic edifice [*Glicken*, 1986; *Siebert*, 2002; *Voight et al*., 1981, 2002; *Masson et al*., 2002, 2006], which may include the *terrestrial* or *submarine flank* of the volcano. A debris avalanche involves considerable disintegration of the edifice material, which results in a poorly sorted blocky deposit with a typically hummocky surface morphology. Debris avalanches are distinguished from *slumps*, which are coherent masses of poorly consolidated materials or rock that move relatively short distances downslope on concave-up or planar slip surfaces [e.g., *Delcamp et al*., 2008]. *Debris flows* are water-saturated flows of disaggregated or reworked sediment with high sediment concentrations and strong interactions between solid and fluid constituents [*Iverson*, 1997]. *Turbidity currents* are rapidly moving, sediment-laden water flows moving down an offshore slope, driven by the density difference between the turbidity current and the clear water above [*Talling et al*., 2012]. Failures of seafloor sediment located beyond the slope break marking the base of the volcanic edifice are referred to as *seafloor sediment failures* [*Watt et al*., 2012a, 2012b, 2014].

2. Overview of IODP Expedition 340–Data

Expedition IODP 340 on the R/V *JOIDES Resolution* drilled and cored in marine sediments and volcaniclastic material at nine sites located off the islands of Montserrat (where the Soufrière Hills volcano has been active since 1995, resulting in serious hazards and significant social impacts), Martinique (with the famous Montagne Pelée volcano that tragically killed about 30,000 inhabitants in 1902) and Dominica (where several large-silicic eruptive centres are considered active and pose serious potential regional hazards and risks due to the occurrence of large magnitude ignimbrite-forming eruptions in the recent geological past [*Lindsay et al*., 2005]) (Figure 1).

The objective of Expedition IODP 340 was to document eruptive activity and edifice collapse for three of the most active volcanic complexes in the Lesser Antilles Arc over the last million years, in order to better understand the constructive and destructive processes. The aims of the Expedition were thus to (1) understand the timing and emplacement processes of landslide deposits, with implications for tsunami hazards; (2) document the long-term eruptive history of some of the Lesser Antilles volcanoes, guide the prognosis of future volcanic activity and document the volcano evolution (cycles of construction and destruction); (3) access critical information on the long-term magmatic evolution of the Lesser Antilles volcanoes; and (4) understand the processes by which sediment is dispersed around volcanic edifices into the deep ocean.

We recovered 434 core sections containing 2384 m of seafloor sediment samples. Information collected included physical properties on cores (thermal conductivity, shear strength, natural gamma ray emissions, P wave, magnetic susceptibility, density), and data obtained in situ by downhole logging operations (gamma rays, P wave, magnetic susceptibility, resistivity) [*Manga et al*., 2012, *Le Friant et al*., 2013, *Lafuerza et al*., 2014, *Wall-Palmer et al*., 2014]. Table 1 summarizes the location and characteristics of each hole at every site. The cores contain some of the most sand-rich sequences yet recovered by IODP, where piston coring disturbances, such as basal flow-in and fall-in, are the most likely to occur [*Jutzeler et al*., 2014]. Particular care was taken to distinguish disturbed from in situ facies. At least two holes were drilled at each site to allow better stratigraphic correlation and minimize coring disturbances (Hole A, Hole B.).

Sites U1396 and U1397 were dedicated to the study of the eruptive history and magmatic evolution of Montserrat [*Wall-Palmer et al*., 2014] and the recent volcanoes of Martinique and South Dominica, respectively (Figure 1). Sites U1393, U1394, U1399, U1400 and U1401 were chosen to study landslide deposits and associated processes (Figures 1–3). Sites U1395 and U1398 were dedicated to study of the differences between the distal sedimentation processes in the north and the south of the arc (Figures 1 and 3).

In this paper we provide initial results for the more specific set of aims as outlined above in section 1.2.

Table 1. Coring Summary, IODP Expedition 340

Hole	Latitude	Longitude	Water Depth (m)	Penetration DSF (m)	Core Interval (m)	Recovered Length (m)	Recovery (%)
U1393A	16°43,1316 N	62°05,0594 W	926	47.5	47.5	5.42	1
U1394A	16°38,4259 N	62°02,2822 W	1114.9	244.5	244.5	57.37	23
U1394B	16°38,4375 N	62°02,2819 W	1114.2	181.4	181.4	141.15	7
U1395A	16°29,5988 N	61°57,0858 W	1200.9	231.3	231.3	144.18	6
U1395B	16°29,5985 N	61°57,0751 W	1200.2	203.3	203.3	140.21	6
U1396A	16°30,4841 N	62°27,1017 W	787.4	134.9	134.9	140.51	10
U1396B	16°30,4847 N	62°27.0912 W	787.4	14.5	9.5	10	105
U1396C	16°30,4729 N	62°27,0905 W	786.6	139.4	139.4	145.92	10
U1397A	14°54.4081 N	61°25,3530 W	2482.2	265.5	261.1	144.2	55
U1397B	14°54,4075 N	61°25,3421 W	2481.4	253.5	248.7	131.46	53
U1398A	14°16.6984 N	61°53,3422 W	2935.3	268.6	268.6	115.09	43
U1398B	14°16,6987 N	61°53,3309 W	2935.1	263.4	263.4	186.75	71
U1399A	14°23,2419 N	61°42,6833 W	2900.8	274.7	274.7	219.88	80
U1399B	14°23,3639 N	61°42,5380 W	2900.2	183	180.5	183.04	10
U1399C	14°23,2593 N	61°42,6665 W	2900.8	240	0	0	
U1400A	14°32,5831 N	61°27,5492 W	2744.4	51.3	51.3	51.8	10
U1400B	14°32,2023 N	61°27,4065 W	2743	212.5	212.5	215.19	10
U1400C	14°32,1935 N	61°27,4028 W	2743	436	421	304.49	72
U1401A	14°39,0991 N	61°25,0797 W	2596.7	81.5	81.5	15.61	19
U1401B	14°39,0237 N	61°25,2273 W	2606.2	12.9	12.9	12.42	96
U1401C	14°39,1744 N	61°24,9323 W	2578.8	10.3	10.3	10.44	10
U1401D	14°38,9463 N	61°25,3743 W	2617.9	9.2	9.2	9.12	9

3. Results

We first describe results from cores obtained through landslide deposits offshore Martinique, then the results from cores offshore Montserrat, and finally observations of the tephra layers and turbidite deposits.

3.1. Landslides Offshore Martinique

Martinique consists of several volcanic centres with a history extending back to about 23 Ma [*Westercamp and Traineau*, 1983, *Germa et al*., 2010]. The evolution of the active Montagne Pelée volcano has been marked by three major flank collapses (at ~ 0.1 Ma, ~ 25 ka and, ~9 ka), which removed much of the western flank of the volcano [*Le Friant et al*., 2003a; *Boudon et al*., 2005, 2007]. Collapse volumes vary from 2 to 25 km^3 and debris avalanches flowed into the Grenada Basin (Figures 1 and 2; Table 2). Three large chaotic landslide deposits (Deposits 1–3) were recognized offshore with high-resolution bathymetry and geophysical data. They display morphological fronts (Deposit 2) and hummocky morphologies (Deposit 3) on bathymetric data, a speckled pattern on backscatter data, and hyperbolic facies on 3.5 kHz and seismic profiles (Deposits 1–3; Figures 2 and 4). The submarine landslide deposits have been traced back to three horseshoe-shaped structures identified on-land. Pitons du Carbet volcano also experienced a large flank collapse 0.35 Ma ago (K-Ar dating) [*Boudon et al*., 1992, 2007, 2013; *Samper et al*., 2008], but although voluminous debris avalanche deposits have been mapped on-land, no correlative offshore landslide deposits have been recognized.

Table 2. Parameters and Ages of the Landslide Deposits Drilled Offshore Montserrat and Martinique During the Expedition IODP 340[a]

Name of Deposit	Surface Area (km^2)	Volume (km^3)	Runout (km)	Ages (ka)
Martinique				
Deposit 3	60	1.6	33	30–45
Deposits 1 and 2	2000	>250	75	70–115
Montserrat				
Deposit 1	51	1.7	12	12–14
Deposit 2	212	9.5	34	138

[a]Data are modified from *Le Friant et al*. [2003a], *Boudon et al*. [2007], *Lebas et al*. [2011], *Watt et al*. [2012b] and completed with this contribution for constraints on ages.

Le Friant et al. [2003a] proposed that the repeated instabilities toward the west on Martinique volcanoes are due to the distinct asymmetry of the island, with western aerial and submarine slopes being steeper than the eastern ones. This asymmetry results from the presence of the back-arc Grenada Basin to the west of the southern islands and the progressive loading by accumulation of volcanic products on the western slopes of the volcano aided by the development of long-term gravitational instabilities. Three sites U1399, U1400 and U1401 were dedicated to investigate the three seismically chaotic landslide deposits offshore Montagne Pelée volcano (Figures 1, 2, and 4).

1. *Site U1399* (Hole A: 274.7 m, Hole B: 183 m, Hole C: 240 m) located on landslide Deposit 1 is associated with the oldest flank-collapse event. Deposit 1 is ~135 m thick at this core site located 78 km offshore from Montagne Pelée volcano (Figures 1, 2, and 4). Lithostratigraphic descriptions show that sediment cored at site U1399 consists entirely of seafloor sediment and is dominated by a combination of hemipelagic mud with interbedded tephra layers and volcaniclastic turbidite deposits (Figures 5 and 6) [*Lafuerza et al*., 2014]. No debris avalanche deposits comprising blocky material from the subaerial volcanic edifice were recognized. The seismically chaotic landslide deposit comprises two types of material. In type 1, stratigraphic intervals up to ~20 m thick, consist of homogenized sediment resembling debris flow deposits with a muddy sand matrix that also can contains large clasts (mud clats and pumice clasts from granules to few centimeters in size). These intervals record intense deformation which, in some cases, has fully homogenized the sediment (Figures 6a and 6b). In type 2, flat-lying or inclined parallel beds (Figure 6c) form intervals that can be up to ~20 m thick. These intervals commonly display small-scale brittle faults, (typically with offsets of only a few cm), but are not as strongly deformed as the type 1 of material (Figure 6). A key observation is that intervals of intense deformation (type 1) occur at multiple depths within this site, i.e., deformation was not focussed only at the base of the landslide deposit. The deformation that occurred between 23 m and 160 m is also split by some nondeformed intervals. Deposit 1 is overlain by 14-to-23 m (depending of the hole) of nondeformed drape that postdates the landslide movement. The age of Deposit 1 may be calculated from drape thickness using estimates of sedimentation rate. However, this sedimentation rate is poorly constrained, varying from ~2 to 8 cm/ka offshore Montserrat [*Le Friant et al*., 2008; *Trofimovs et al*., 2013] to > 20 cm/ka in parts of the Grenada Basin [*Reid et al*., 1996]. Assuming a sedimentation rate of ~20 cm/ka this suggests an approximate age of 70–115 ka, although with very large uncertainties.

2. *Site U1400* (Hole A: 51.3 m, Hole B: 212.5 m, Hole C: 436 m) penetrates through volcanic and biogenic sediment that is intercalated with the large-scale landslide Deposits 1 and 2, 46 km offshore Montagne Pelée volcano, (Figures 1 and 2). The site is dominated by a combination of hemipelagic mud with thinly interbedded tephra layers and volcaniclastic turbidite deposits, representing seafloor sediment rather than debris avalanche deposits. Many of these planar beds are inclined with an average dip of 40°, but some dip as steeply as 70°. These intervals broadly resemble type 2 deposits at Site U1399 and contain a few microfractures. Intervals of homogenized sediment (type 1 deposits) are rare at Site U1400. The boundary between Deposit 1 and Deposit 2 cannot be identified unambiguously in these cores, as there is no difference between the composition of the two landslides. We thus refer to a single depositional unit that we called Deposit 1-2. The base of the deformed sequence is located at 390 m below sea level floor (mbsf), and below this depth, the recovered material consists mainly of hemipelagic mud and partly lithified mudstone that lack any signs of sediment deformation.

3. Site *U1401* (Hole A: 81.5 m, Hole B: 12.9 m, Hole C: 10.3 m, hole D: 9.2 m) is located 35 km offshore from Montagne Pelée volcano, on landslide Deposit 3 which has a hummocky morphology and is associated with the most recent flank-collapse event of Montagne Pelée volcano (Figures 1 and 2). Drilling conditions did not allow penetration into the blocky landslide Deposit 3, and the core was limited to the sedimentary sequence that overlies Deposit 3. This section consists of a combination of hemipelagic mud with interbedded tephra layers and/or volcaniclastic turbiditic deposits [*Le Friant et al*., 2013], with the latter being particularly coarse-grained at the base of the core, including coarse sand and mafic andesite clasts (few centimeters) as well as gravels which could have been produced by drilling into larger blocks. The age of Deposit 3 may be calculated from drape sediment thickness (9 m in hole D, 14 m in hole A) using previous estimates of sedimentation rate >20 cm/ka offshore Martinique [*Reid et al*., 1996; *Boudon et al*., 2013]. Assuming a maximum sedimentation rate of 30 cm/ka, this suggests an approximate age of 30–45 ka for Deposit 3, although with very large uncertainties. This age is older than the previous age proposed [*Le Friant et al*., 2003a].

3.2. Landslides Offshore Montserrat

Volcanism migrated from north to south on Montserrat, forming a series of volcanic centres (Figure 3) [*Harford et al*., 2002]. The eruption of Soufrière Hills volcano, which started in 1995 [*Druitt and Kokelaar*, 2002; *Wadge et al*., 2014], shows a succession of different eruptive styles with lava dome growth and vulcanian

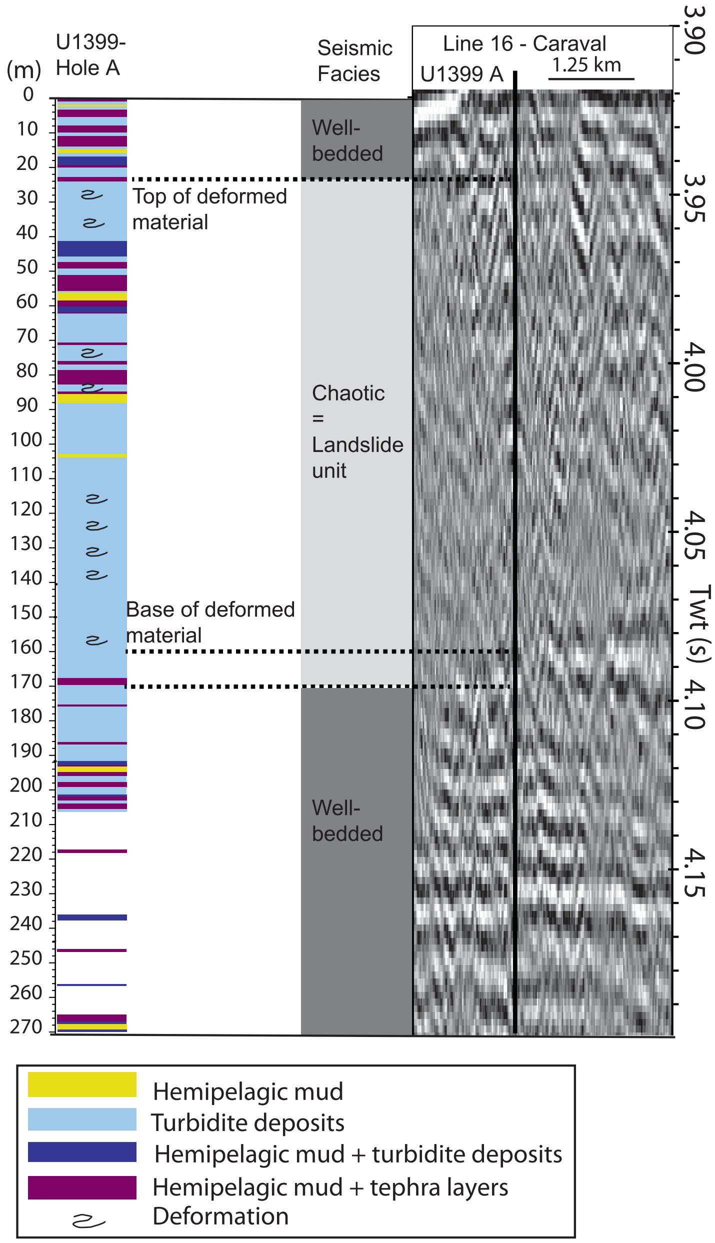

Figure 5. Summary of lithology of Hole 1399A offshore Martinique (through Deposit 1) and correlation with seismic reflection data (Line 16–Caraval). Chaotic unit and deformed unit are annotated both on reflection profiles and cores respectively. White areas indicate cores without recovery.

explosions generating abundant pyroclastic density currents. Most of the pyroclastic density currents entered the sea, where their deposits have also been studied in detail [*Le Friant et al.*, 2009, 2010; *Trofimovs et al.*, 2006, 2008, 2010, 2013; *Cassidy et al.*, 2013]. Minor tsunamis were sometimes caused by the rapid entrance of volcanic material into the sea [*Sparks et al.*, 2002; *Mattioli et al.*, 2007].

Several prehistoric flank collapses have been recognized on Soufrière Hills volcano as well as a series of large submarine landslide deposits around the island [*Le Friant et al.*, 2004; *Lebas et al.*, 2011, *Watt et al.*, 2012a, 2012b; *Crutchley et al.*, 2013; *Karstens et al.*, 2013] (Figure 3). The horseshoe-shaped English's Crater was probably formed at ~12–14 ka and is likely related to Deposit 1 [*Trofimovs et al.*, 2013]. In addition, smaller recent collapses have been recognized at 2 ka and 6 ka leading to turbidite emplacement offshore Montserrat [*Le Friant et al.*, 2004; *Boudon et al.*, 2007, *Trofimovs et al.*, 2013[. Two of the 10 submarine landslide deposits identified offshore Montserrat by *Lebas et al.* [2011] were drilled by Expedition 340 to the

Figure 6. Deformation observed within the cores: (a) Convolutes, U1399A (depth: 25.40m); (b) Mixing, U1400C (depth: 25.05 m); (c) Inclined layers and microfaults; U1400C (depth: 34.95 m).

southeast of Montserrat (Deposits 1 and 2; Table 2). Submarine landslide Deposit 1 has a very hummocky morphology and a chaotic signature on seismic profiles (Figure 3). *Lebas et al*. [2011] noticed that the volume of Deposit 1 (~1.7 km^3) exceeds that of the associated subaerial collapse scar ~0.5 km^3). *Trofimovs et al*. [2013] suggest a substantial involvement of a submerged carbonate shelf around Montserrat. The older landslide (Deposit 2) is much more extensive and voluminous (~20 km^3) but has a much less blocky character than landslide Deposit 1 (Figure 3). Much of Deposit 2 has a smooth upper surface which, together with the presence of internal reflectors and a lateral transition into well-bedded seismic units at its margins, suggests that most of the landslide volume comprises preexisting seafloor sediment [*Watt et al*., 2012a, 2012b]. Deposit 2 therefore resulted from a combined submarine and subaerial landslide process of the eastern flank of the volcano that included failure and deformation of submarine sediment [*Le Friant et al*., 2004; *Lebas et al*., 2011; *Watt et al*., 2012a, 2012b, 2014].

1. *Site U1393* (Hole A: 47.5 m) was located to sample landslide Deposit 1, 10 km offshore Soufrière volcano. Due to the heterogeneity, coarse grain size and unconsolidated nature of the chaotic Deposit 1, attempts to drill through the deposit were unsuccessful. The main lithologies cored at Site U1393 from the upper 47.5 m of stratigraphy are hemipelagic mud, turbiditic sand and mud, mafic volcaniclastics and tephra deposits overlying the chaotic deposits [*Le Friant et al*., 2013].

2. *Site U1394* (Hole A: 244.5 m, Hole B: 181.4 m) is located on landslide Deposit 2, 17 km offshore Soufrière volcano. The main lithologies cored are hemipelagic mud, turbiditic sand and mud and few tephra layers such as mafic volcanic deposits (Figures 7 and 8) [*Le Friant et al*., 2013]. The upper part of Deposit 2 was not recovered, but there was continuous recovery of its lower half. The turbidite units in Deposit 2 are generally thicker (ten to several tens of centimeter) that those seen at Site U1400, even allowing for suck-in of sand by basal flow-in during piston coring [*Jutzeler et al*., 2014]. The landslide unit, which corresponds to the chaotic, or sometimes locally bedded, seismic reflectors (Figure 7), is dominated by a stacked sequence of predominantly thick, massive, relatively coarse-grained turbiditic deposits that range in composition from bioclastic to volcanoclastic (Figures 7 and 8). Surprisingly, especially when compared to the Martinique sequences, the layers recovered from the landslide deposit at Site U1394 are entirely flat-lying and planar, showing no signs of deformation. It appears, therefore, that they represent a block of intact stratigraphy within the landslide. A series of basaltic tephra layers directly overly landslide Deposit 2 and correlate to subaerial basaltic fallout deposits associated with the South-Soufrière Hills volcano, dating back to 138 ka, thus providing a minimum age for Deposit 2. No debris avalanche deposits were observed at Site U1394.

3.3. Tephra and Turbidite Deposition Adjacent to Volcanic Islands

Most of the volcaniclastic material originating from the volcanoes of the Lesser Antilles arc is transported into the surrounding ocean [*Le Friant et al*., 2010]. Hence, four drilling sites were dedicated to volcano history reconstruction and sedimentation within the adjacent basins: two offshore Montserrat (Figure 3) and two offshore Martinique and Dominica (Figures 1 and 2). These drilling sites also aimed to capture longer runout flow deposits generated by major landslides.

1. *Site U1395* (Hole A: 231.3 m, Hole B: 203.3 m) is located beyond the furthest extent of the landslide deposit identified on the seismic reflection lines within the Bouillante-Montserrat half-graben (Figures 1 and 3) [*Feuillet et al*., 2010]. The recovery rate was close to 100% and the material cored consists of tephra layers and mixed bioclastic-volcaniclastic turbidites interbedded with hemipelagic background sediment probably originating from Montserrat. In addition, some of the tephra fall deposits and turbidite deposits probably originate from volcanoes of the northern and central parts of Guadeloupe (Figure 1). The magnetostratigraphy suggests sedimentation rates of 9 cm/ka within the Bouillante-Montserrat half-graben, contrasting with the 3.1 cm/ka recorded in U1396, due to the greater abundance of turbidites within the graben. For example, this site contains a 7 m thick turbidite unit correlated with emplacement of landslide Deposit 2, which is the subject of further study.

2. *Site U1396* (Hole A: 134.9 m, Hole B: 14.5 m, Hole C: 139.4 m) is located on a topographic high, west of Montserrat (Figure 1). The sedimentary sequence comprises a series of hemipelagic sediment, tephra layers and volcanoclastic mud. At least 180 tephra layers of varying thickness are intercalated in the hemipelagic background sedimentation and there might be many more cryptotephra layers embedded in the hemipelagic mud [*Le Friant et al*., 2008]. Preliminary biostratigraphic studies combined with the magnetostratigraphic record assign the lowest recovered cores to late Pleistocene to early Pliocene ($\sim$4 to 5 Ma) [*Le Friant et al*., 2013]. This drilling site allowed us to reconstruct a long-term eruptive history of Montserrat, with a particularly detailed analysis of events during the last 250 ka at this location [*Wall-Palmer et al*., 2014].

3. *Site* U1397 (Hole A: 265.5 m, Hole B: 263.5 m) is located on a topographic high bound by large canyons west of Martinique (Figure 1). Sediments retrieved at this site consist of various combinations of hemipelagic mud, volcaniclastic or mixed (i.e., volcaniclastic-bioclastic) turbiditic deposits and tephra layers. The proportion of tephra layers and volcaniclastic turbidites is higher than in U1396 and will be crucial to reconstruct the volcanological history from north Martinique (Montagne Pelée and Pitons du Carbet) and south Dominica. For example, 200 tephra layers have been recognized in the first $\sim$30 m of the cores [*Le Friant et al*., 2013]. At the base of the core, some lava clasts suggest lithologies characteristic of Pitons du Carbet volcano and indicate a minimum age of 320 ka, which represents the end of activity at this volcano, [*Samper at al*., 2008; *Germa et al*., 2010].

4. *Site U1398* (Hole A: 268.6 m, Hole B: 263.4 m) is located in the back-arc Grenada Basin, west of Martinique. Volcaniclastic turbiditic deposits dominate the upper part of the site, whereas hemipelagic mud with intercalated volcaniclastic turbiditic deposits and tephra layers characterize the lower parts. Voluminous turbiditic deposits, up to 10 m thick, are recognized, and contribute to the large sedimentation rates in the Grenada Basin ($>$ 20 cm/ka). The lava lithologies indicate that most of the turbiditic deposits probably originated from Dominica.

3.4. Seismic Velocities Within Sediments Around Volcanic Islands

An additional objective of Expedition 340 was to better characterize the seismic velocities of the different materials deposited around the Lesser Antilles arc (e.g., marine background sediment versus volcaniclastic material). This would allow reanalysis of the original seismic data. P-wave measurements from both whole-round sections and split sections show velocities ranging from 1500 to 1900 m/s. Generally, higher velocities (1650 to $>$ 1800 m/s) are obtained from the volcanic layers, while lower velocities characterize the hemipelagic background sediment (1550–1650 m/s). Table 3 presents mean velocities measured for each drilling site, although such values may be biased low because of coring disturbance. The measurements of seismic velocities within recovered material allow us to correlate seismic reflection profiles obtained during several preceding cruises (Aguadomar-1999, Caraval-2002, Gwadaseis-2009, JR45/46–2010) with cored material. These data were particularly useful in refining estimates of the thickness of the chaotic units, which were previously estimated with assumed velocities of 1800 to 2200 m/s [e.g., *Urgeles et al*., 1997; *Le Friant et al*., 2003a].

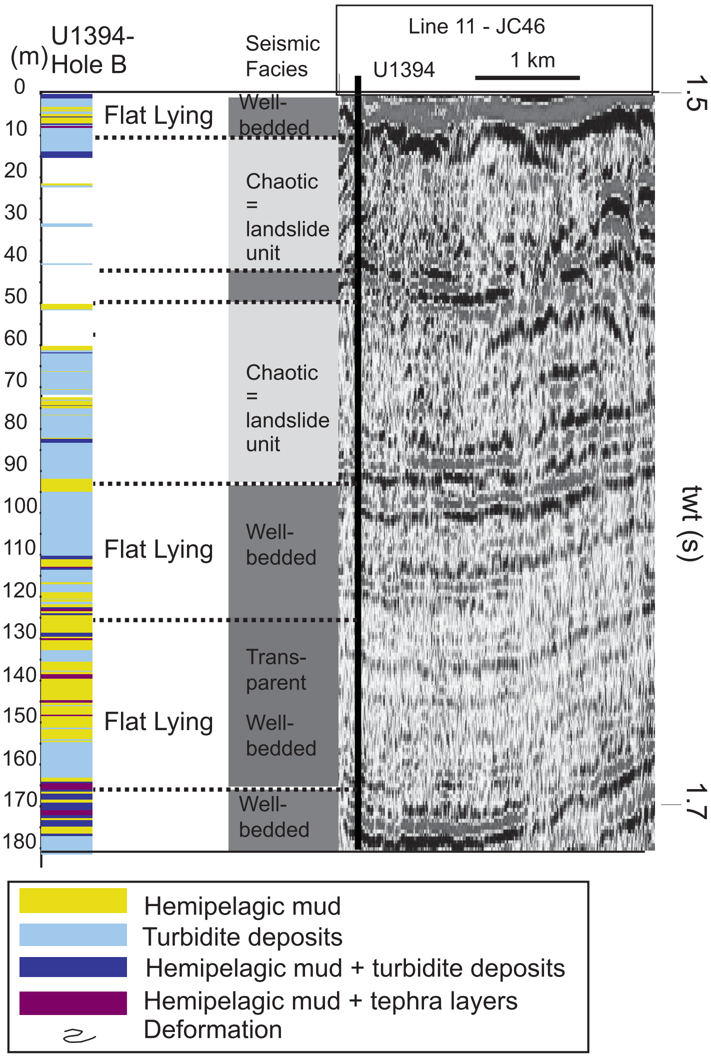

Figure 7. Summary of lithology of Hole 1394B offshore Montserrat (through Deposit 2) and correlation with seismic reflection data. Chaotic unit and deformed unit are annotated both on reflection profiles and cores respectively.

4. Discussion

While we only report data on a small number of sites, drilling through the seismically chaotic deposits offshore Lesser Antilles volcanoes identified by previous seismic profiles has revealed some important insights.

4.1. Blocky Volcanic Debris Avalanche Deposits

Deposits with very blocky surface morphologies (Site U1393 and U1401) were difficult to drill, probably due to prevalence of hard drill-resistant lava blocks in the poorly sorted heterogeneous material. The examples include Deposit 1 at Site U1393 offshore Montserrat and Deposit 3 at Site U1401 offshore Martinique (Figures 1–3). These landslide deposits are located on the submarine flanks of the volcanoes or around the slope break between the submarine flanks and surrounding basins. They are most likely debris avalanche deposits composed of cohesionless poorly sorted blocky material derived from different volcanic edifices, or submarine flank lithologies although this interpretation remains unconfirmed by our drilling.

4.2. Large Landslide Deposits Dominated by Seafloor Sediment

Seismically chaotic deposits were successfully drilled on sites U1394, U1399, U1400 and revealed the absence of volcanic debris avalanche deposits, although the mechanisms producing these deposits may have been triggered by subaerial or submarine volcanic flank-collapses. The chaotic units consist of a combination of hemipelagic mud, volcanoclastic and bioclastic turbiditic deposits and tephra layers. Offshore

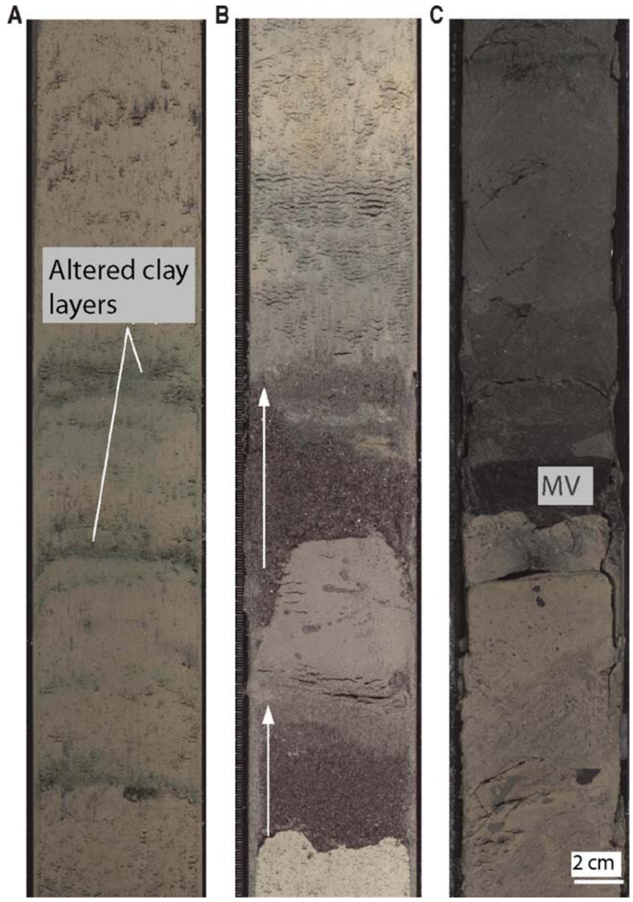

Figure 8. Photographs of Site U1394 core sections. (a) Hemipelagic mud, U1394A (depth: 4.40 m); (b) Turbiditite sequences with fining-upward trends indicated by arrows, U1394B (depth: 3.90 m); (c) Mafic volcanicalstic deposits, U1394A (depth: 168.70 m).

Martinique, the chaotic units are located in front of the subaerial horseshoe-shaped structures created by the aerial flank-collapse events. This is also true for Montserrat, with some offshore headscarps (and adjacent slump blocks) clearly indicating failure of offshore sediment in Deposit 2 [*Watt et al.*, 2012a, 2012b]. Given the spatial relationship between deposits and collapse scars, our new core data on the composition of landslide deposits allows us to test, for the first time, previous hypotheses for models for volcanic landslide emplacement, such as those of *Deplus et al.* [2001] and *Watt et al.* [2012a, 2012b] (Figure 9). These four hypotheses are outlined and discussed below.

4.2.1. Hypothesis A: Erosion and Loading of Seafloor Sediment by Volcanic Debris Avalanche

Deplus et al. [2001] suggested that the seismically chaotic deposits interpreted as submarine landslides deposits could be directly related to subaerial flank-collapses (Figure 9a). Lacustrine sediments that have been prominently deformed by the emplacement of debris avalanche at Jocotitlan volcano have been described by *Siebe et al.* [1992] and *Dufresne et al.* [2010]. Volume discrepancies between on-land scarps structures and offshore deposits were proposed to be due to erosion by the debris avalanches which incorporated and disturbed underlying weak layers of seafloor sediment. *Deplus et al.* [2001] proposed that the upper part of the seismically chaotic landslide deposits would comprise a mixture of material from the volcanic edifice and entrained seafloor sediment, while the lower part of the landslide deposit would consist mainly of deformed seafloor sediment (Figure 9a) [*Deplus et al.*, 2001]. However, some of our distal cores (U1394, U1399, U1400) through seismically chaotic deposits exclusively comprise seafloor sediment, with variable types of deformation that extend to the upper boundary of the deposit. It thus appears that original volcanic debris avalanches did not reach the more distal landslide core sites, discounting possible transformation of some of this material to debris flow. This result suggests that the runout distance of the volcanic debris avalanche was not as far as previously thought (i.e., less than 37 km offshore Martinique), but also suggests that mobilized sea floor sediment forms the bulk of the more distal facies of the deposit.

4.2.2. Hypothesis B: Loading of Seafloor Sediment by an Overrunning Volcanic Debris Flow

Watt et al. [2012a, 2012b] suggested that a debris flow runs out beyond the limits of the primary debris avalanche, slides over the underlying seafloor, and loads the underlying undrained seafloor, such that it deforms and fails, (Figure 9b1). A variant of this model is that transmission of significant, quasi-continuous shear stress from an overrunning volcanic sediment flow to the underlying seafloor sediment causes coupled deformation of seafloor sediment (Figure 9b2). Note that the cases B1 and B2 are really end-member cases. In B1, the overriding debris flow may have low shear coupling throughout most of its transport, but as it comes to rest the shear traction increases, and overall the loading therefore includes both a normal load component and a time-variable shear traction component. Failure of seafloor sediment could involve limited decollement slip and shear on multiple horizons. The distinction between cases B1 and B2 is whether the application of significant shear traction is quasi-continuous with debris flow runout and emplacement (case B2), or whether significant shear traction is limited to the final stages of emplacement (case B1).

Offshore Martinique, lack of evidence of an overrunning volcanic flow at Sites U1399 and U1400 suggests that such models cannot explain the large submarine landslide deposits at that location. Offshore Montserrat, at Site U1395, a 7 m-thick turbidite deposit rich in volcanic material appears to be associated with landslide Deposit 2 emplacement. This suggests that a powerful overrunning debris flow occurred at this site, supporting the viability of the case B mechanisms. However, there is no evidence that the seafloor sediment was deformed by shearing (or indeed other processes) along its upper boundary.

4.2.3. Hypothesis C: Self-Loading by Down-Slope Propagating Seafloor Sediment Failures

This model proposes that emplacement of the initial debris avalanche imposes a lateral load on adjacent, undrained seafloor sediment causing localized shear failure (Figure 9c). The slice of sheared seafloor sediment then loads an adjacent area of seafloor sediment that also fails, in turn loading the next area of the seafloor [*Watt et al*., 2012b]. This hypothesis does not require the imposition of shear tractions from an overrunning avalanche or debris flow.

The model is consistent with the lack of volcanic debris avalanche material at the sites cored by Expedition 340. This model also predicts that there should be local areas of both intact and tilted stratigraphy, and is thus consistent (but not exclusively) with the presence of an intact block within landslide Deposit 2 seen offshore Montserrat at Site U1394, and the areas of tilted stratigraphy observed offshore Martinique at Sites U1399 and U1400.

4.2.4. Hypothesis D: Decollement Propagation From Debris Avalanche Deposit Loading

The last model suggests that debris avalanche deposit loading could initiate decollement (fracture) propagation away from the site of initial failure. Previous modeling suggests that local failure can generate cracks that propagate very rapidly over much wider areas than the initial site of failure, in a similar way to thrust-fault and decollement mechanics, and snow slab avalanches [*Viesca and Rice*, 2012]. Lateral propagation can occur even where the load of the debris avalanche (vertical effective stress) is not fully supported by excess pore pressure in the undrained sediment, such that these parts of the slope were not originally prone to failure (Figure 9d). In addition, lateral loading produced by the debris avalanche, which may have eroded in to the seafloor, can also promote overpressure (Figure 9d). Basal decollement could thus propagate laterally from emplaced volcanic debris avalanche, to produce widespread deformation of seafloor sediment above the decollement (Figure 9d). This process could explain why the IODP 340 core sites did not encounter any volcanic debris avalanche material in the seismically chaotic landslide deposits, and why there appears to be a block of undeformed strata in landslide Deposit 2 at Site U1394 offshore Montserrat.

Table 3. Mean Sediment Seismic Velocity (m/s) and Standard Deviations

	Depth (m)	Mean Velocity (m/s)	Standard Deviation (m/s)
U1393A	0–4 m	1718	119
U1394A	0–208 m	1604	152
U1394B	1–181 m	1609	77
U1395A	0–175 m	1570	80
U1395B	0–153 m	1588	69
U1396A	0–135 m	1588	20
U1396B	0–15 m	1589	30
U1396C	0–139 m	1564	46
U1397A	0–257 m	1619	109
U1397B	0–238 m	1614	113
U1398A	0–222 m	1629	118
U1398B	0–254 m	1622	102
U1399A	0–268 m	1609	94
U1399B	0–181 m	1602	105
U1400A	0–50 m	1662	110
U1400B	0–209 m	1594	64
U1400C	0–410 m	1594	73

Model D might be expected to produce areas of extension, and thus extensional faults closer to source. However, it is also possible that such faults might be buried by late-stage debris avalanche deposition. Such extensional faults are not observed in seismic data offshore Montserrat. Seismic reflection profiles offshore Martinique are not of high resolution for the proximal part on the flank of the volcano, but the presence of some extensional structures (normal faults) has been suggested.

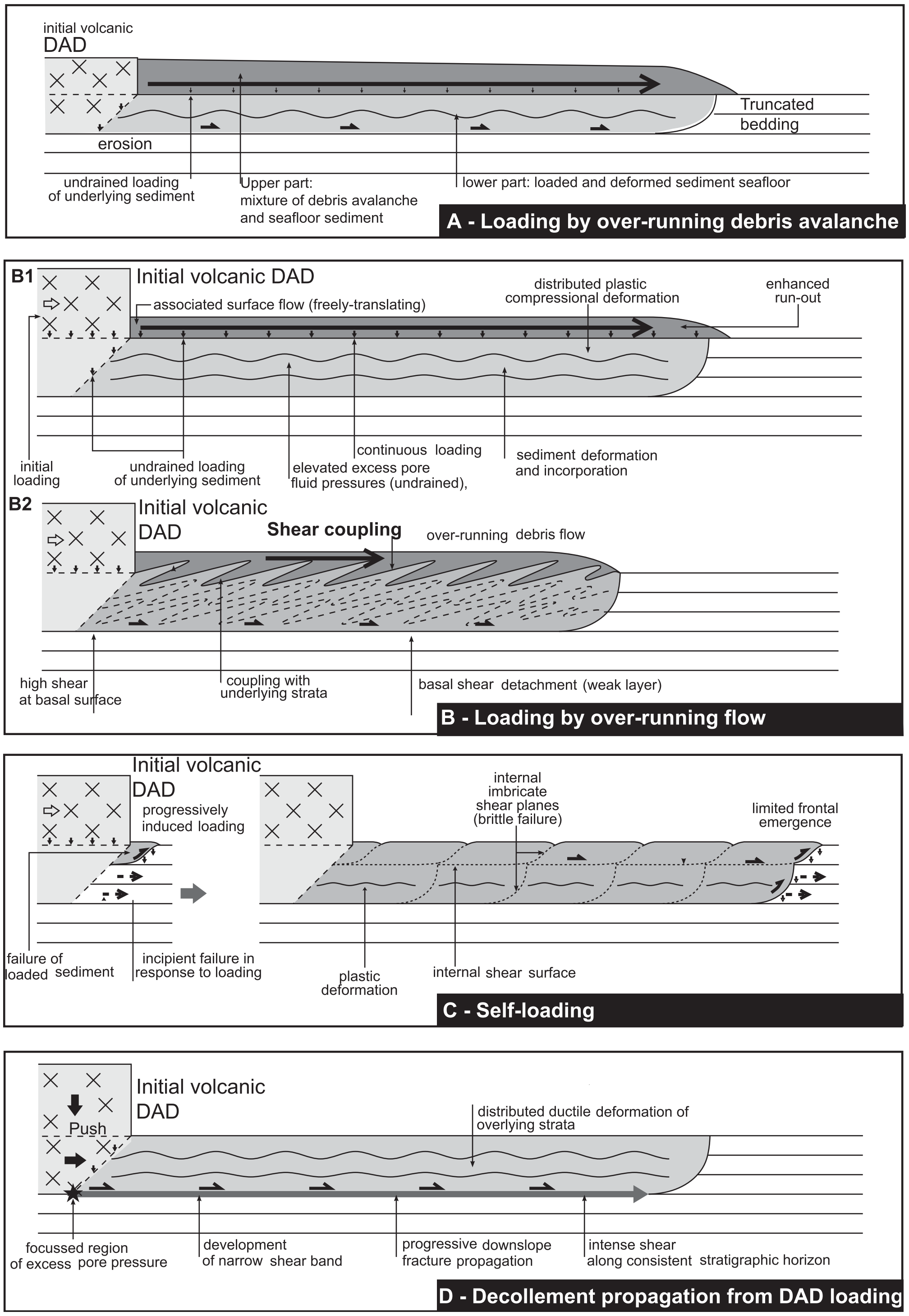

Figure 9. Summary of models for the emplacement history and resulting composition of landslide deposits offshore from volcanic islands. (a) Loading by overrunning debris avalanche. An initial volcanic debris avalanche erodes into the seafloor sediment to form a two-layer deposit. The upper layer in the landslide deposit comprises a mixture of material from the volcanic edifice and seafloor sediment, whereas the lower part of the landslide deposit is exclusively composed of seafloor sediment. From *Deplus et al.* [2001]. (b) Loading by overrunning flow. (b1) An initial volcanic debris avalanche forms a longer runout debris flow, which loads and causes deformation in underlying seafloor sediment. (b2) Shear coupling between an overrunning flow (turbidity current or debris flow) causes deformation of underlying seafloor sediment, modified from *Watt et al.* [2012b]. (c) Self-loading. Initial failure of seafloor sediment loads the adjacent seafloor area in a downslope direction, causing deformation to migrate downslope, modified from *Watt et al.* [2012b]. (d) Shear rupture propagation. A shear rupture (fracture) surface propagates downslope from the location of initial volcanic debris avalanche emplacement. In addition, the initial volcanic debris avalanche may have incised into the seafloor and imparted a strong lateral force on a layer of seafloor sediment.

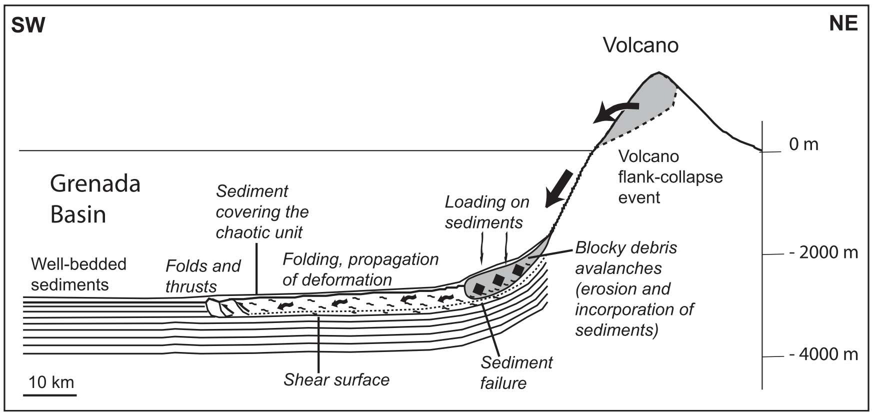

Figure 10. Schematic figure of processes that can explain the presence of huge landslide deposits offshore volcanic islands (topographic/bathymetric profile from Martinique). Volcano flank-collapses generate debris avalanches that enter the sea, incise the sediments and generate failure, propagation and deformation of marine sediments.

Additional higher resolution seismic profiles may be needed to identify such areas of extension offshore Martinique.

4.2.5. Summary

To summarize, Model A "loading of seafloor by volcanic debris avalanche" is not consistent with observations offshore Martinique and Montserrat. Model B "shear traction caused by overrunning debris flow" could be compatible with observations of Deposit 2 from Montserrat but does not correlate with results from Martinique. Model C "self-loading" could be viable but raises the question of whether the continued failure is due to localized "self-loading" of only the small failed slice. From our observations, the most likely mechanism for these large-scale distal seafloor sediment failures (comprising the seismically chaotic landslides) appears to be model D in which the decollement propagates from proximal areas loaded and incised by volcanic debris avalanche emplacement (Figures 9d2 and 10). This model may also explain the large-scale landslide deposits observed in the southern part of the Lesser Antilles from Dominica to St-Vincent; if so, this process may operate over the whole length of the arc (Figure 1).

4.3. Differences Between Landslides Offshore Martinique and Montserrat

Although landslide deposits in the distal parts offshore Montserrat and Martinique were both found to comprise exclusively seafloor sediment rather than volcanic debris avalanche deposits, there are significant differences between the drilled cores. In particular, broadly undeformed stacked turbiditic deposits were recovered offshore Montserrat, whereas deformed sediment including mud, tephra layers and turbiditic deposits were recovered offshore Martinique. Most notably, there is a complete lack of deformation within the lower part of landslide Deposit 2 offshore Montserrat, suggesting that it is a nearly intact block although it might have experienced limited displacement. It is difficult, however, to assess whether greater deformation occurs away from this single drilling site through Deposit 2 offshore Montserrat. The landslide deposits offshore Martinique contain a high component of tilted or microfaulted parallel bedded strata, with fully or partially homogenized layers at the U1399 core site. Further cores would be necessary to capture any spatial variability in the landslide deposit but the combination of the larger-scale, the greater relief (4400 m, from summit of the volcano to the Grenada Basin floor) and the steeper slopes involved in the Martinique landslides may have led to greater deformation of seafloor sediment within the deep back arc Grenada Basin.

4.4. Importance of Turbidity Current Deposits and Implication for Sedimentation

An additional aim of IODP Expedition 340 was to assess the various styles of depositional processes offshore these volcanic islands. Analysis of the cores reveals the clear importance of turbidity currents with abundant turbidite deposits observed in the Grenada Basin offshore Martinique, and in the Bouillante-Montserrat half graben offshore Montserrat. In the southern part of the arc (Grenada Basin), the turbiditic deposits are dominant in the upper part of the drilling site, where they can reach 10 m of thickness (site U1398). The turbidite deposits are mainly volcaniclastic in composition and are more abundant at site U1398 than at site U1400. In the northern part of the arc (Bouillante-Montserrat half graben), the turbidite deposits are dominated by carbonates. This is most likely due to the greater extent of the carbonate shelf around the islands in this area (e.g., north of Montserrat, Antigua), so that there is more extensive erosion and incorporation of bioclastic material during erosion along the flow path [*Trofimovs et al*., 2013]. Preliminary biostratigraphic studies of site U1399 in the south suggest that bulk sedimentation rates are much higher (>20 cm/kyr) compared with those observed in the north of the arc (U1395, 9 cm/ka), mainly as consequence of the higher frequency and greater thickness of turbidites at site U1398, which is consistent with previous studies [*Reid et al*., 1996].

4.5. Implications for Tsunami Hazards

Our IODP Expedition 340 results confirm that landslides around Lesser Antilles volcanoes may involve two fundamentally different processes: volcano flank collapse generating blocky debris avalanche submarine deposits (Deposit 1 offshore Montserrat and Deposit 3 offshore Martinique) and seafloor failure generating the large submarine landslide deposits (Deposit 2 offshore Montserrat and Deposits 1, 2 offshore Martinique). Both types of landslide may generate a tsunami, but the magnitude of landslide-derived tsunamis is a source of ongoing debate [*Ward and Day*, 2001; *Masson et al*., 2006; *Watt et al*., 2012a]. Precise estimates of tsunami magnitude are hampered by a lack of direct measurements for key input parameters, such as landslide velocity and initial acceleration.

However, *Watt et al*. [2012a] summarize the approximate magnitudes of tsunami that might be expected for different volume landslides originating from failure of (i) the subaerial volcano, (ii) the submerged slopes of the volcano, or (iii) seafloor sediment in deeper water around the volcano. This analysis was based around Deposits 1 and 2 offshore Montserrat. The analysis used a series of previously proposed relationships based on theory or extrapolation of small-scale laboratory experiments, whose (often considerable) assumptions are discussed in more detail by *Watt et al*. [2012a]. A key general point is that tsunami magnitude depends strongly on the relative speeds of the landslide and tsunami wave, with tsunami magnitude increasing if the tsunami wave travels at a similar speed to the submerged landslide. Similar speeds of the two waves will typically occur only in shallow ($< \sim$200 m) water depths, and this means that seafloor sediment failures located in deep water tend to produce much smaller magnitude tsunamis [*Ward*, 2001]. The analysis of *Watt et al*. [2012a] suggested that a failure of seafloor sediment with a volume of $\sim$2 km^3, would produce a tsunami with a maximum amplitude that is approximately 100 times smaller than a similar volume failure of the subaerial or submerged flanks of the volcano [see *Watt et al*., 2012a, Figure 7]. Even if the failure of seafloor sediment has a much larger volume (e.g., 25 km^3 in Deposits 1 and 2 offshore Martinique; Table 1), it is still likely to produce a much smaller tsunami amplitude than failure of a subaerial or submerged edifice.

The *Watt et al*. [2012a] analysis of tsunamis from seafloor sediment failure is based on wave-tank experiments with a sliding block [see *Watts et al*., 2005]. Such a sliding block model may not, however, capture the way in which deformation propagates within the seafloor sediment offshore Montserrat and Martinique, as depicted within Figure 9. It may be that deformation in seafloor sediment failures is slow moving compared to a sliding block, and that individual parcels of seafloor sediment move lateral for short distances (Figure 9). If this is the case, such slow velocities and short particle-transport distances could further decrease the magnitude of tsunamis generated by seafloor sediment failures. The completely intact block of seafloor sediment recovered at Site U1394 offshore Montserrat is consistent with relatively slow and limited lateral movement of the landslide. In the Martinique landslides, deformation of seafloor sediment appears to occur at multiple horizons within the landslide deposits, which may indicate somewhat more vigorous motion.

A tsunami wave produced by widespread seafloor failure may produce a longer wavelength tsunami than that associated with localized failure of the volcanic edifice. These longer tsunami wavelengths from seafloor sediment failures could act to increase the runout distance of the tsunami, increasing tsunami risks [*Watt et al*., 2012a]. However, even if the volume of flank-collapse is smaller than volume of seafloor sediment failure, it may be the most significant in terms of causing tsunami damage on nearby coastlines.

4.6. Comparison With Landslides Around Other Volcanoes

Collapse of volcanic island flanks has produced some of the largest landslide deposits on Earth's surface. The largest volcanic islands landslides occur in intraplate settings, sometimes with volumes of several hundred or even thousands of cubic kilometers [*Moore et al*., 1989; *Masson et al*., 2002]. The scale of those events far exceeds the largest known subaerial volcanic landslide deposit of Mount Shasta (volume >45 km^3) [*Crandell*, 1989]. Criteria for the identification of offshore landslide deposits have been developed by several authors in different geographical areas [e.g., *Moore et al*., 1989; *Masson et al*., 2002; *Deplus et al*., 2001]. Typically, landslide deposits can display chaotic seismic reflectors with strong energy diffraction, which contrasts with subhorizontal reflectors corresponding to underformed parallel-bedded sediments. An interesting result from sampling of seismically chaotic landslides by Expedition 340 is that they can sometimes be characterized locally by limited (Sites U1399 and 1400 off Martinique), or no visible deformation (Site U1395 offshore Montserrat).

Watt et al. [2014] brought together a range of recent morphological, structural, and sedimentatological observations from previous reviews of volcanic-island landslides [*Moore et al*., 1989; *Deplus et al*., 2001, *Masson et al*., 2002] and more recent data [*Watt et al*., 2012a, *Hunt et al*., 2011] to summarize understanding of how volcanic island landslide deposits were emplaced in disparate locations. The most block-rich volcanic island landslides such as Nuuanu, Hawaii [*Moore and Clague*, 2002] are dominated by kilometer-scale blocks that have slid to their site of deposition. The dominance of angular, intact blocks in some submarine debris-avalanche deposits suggests a relative damping of fragmentation in the submarine environment. In the Lesser Antilles, such angular blocky deposits are observed offshore Dominica. *Watt et al*. [2014] proposed that in several instances the seafloor sediment substrate probably fails during emplacement of a volcanic landslide (Antilles: *Deplus et al*. [2001]; Papua New Guinea: *Silver et al*. [2009]; Aleutian: *Montanaro and Beget* [2011]). This sediment failure remains almost in situ as a deformed package. Moreover, limited lateral transport distances are implied by the geometry of these seafloor sediment failures, as the toe of landslide transitions does not emerge above the seafloor [*Frey-Martinez et al*., 2006; *Watt et al*., 2014]. When the seafloor sediment becomes more disaggregated and no longer confined within the region of initial disruption, a debris flow can propagate for hundreds of kilometers from the location of initial debris avalanche emplacement, as observed for the Canary debris flow that was triggered by the El Golfo debris avalanche [*Masson et al*., 2002; *Hunt et al*., 2011]. Expedition 340 IODP data confirm that chaotic units observed in seismic data do not necessarily represent extensively disaggregated or deformed material, which has been transported for long distances from the volcanic edifice [cf. *Gafeira et al*., 2010]. It supports the view that extensive seafloor sediment failures may be relatively commonplace around volcanic islands [*Watt et al*., 2012a, 2014].

IODP Expedition 340 represents the first successful drilling of volcanic island landslides, showing that such drilling may be feasible elsewhere. The seismic velocities measured by Expedition 340 may be used as benchmark for studies of other volcanic areas with similar chaotic deposits, to yield more accurate interpretations. Such new data are important for improved assessment of volcano and tsunami hazards associated with volcanic-islands landslides.

5. Conclusion

IODP Expedition 340 successfully collected 2.384 km of cores over 9 sites offshore Montserrat, Martinique and Dominica, including some of the most sand-rich core intervals yet recovered by IODP. This demonstrates how IODP drilling can be applied successfully to novel geological settings. IODP Expedition 340 now provides some of the few deep cores located offshore from volcanic islands, and represents the first scientific drilling of volcanic-arc island landslide deposits.

It is important to understand the composition, source and emplacement dynamics of volcanic island landslides, because these factors contribute a significant part of the epistemic uncertainty regarding modeling and forecasting of the initial magnitude of associated tsunamis. The IODP Expedition 340 cores allowed us to carry out the first test of previous hypotheses on the composition and internal morphology of volcanic island landslide deposits (Figure 9) [*Deplus et al*., 2001; *Le Friant et al*., 2004, *Lebas et al*., 2011; *Watt et al*., 2012a, 2012b, 2014]. The IODP Expedition 340 sites (U1394, U1399, and U1400) that successfully penetrated volcanic island landslide deposits recovered exclusively seafloor sediment, comprising mainly of parallel bedded turbidite deposits (volcanoclastic and bioclastic turbidite units) and hemipelagic mud. Notably, these landslide deposits lacked debris avalanche deposits sourced from adjacent subaerial volcanic edifices, suggesting that the runout of those debris avalanche themselves was relatively limited (the debris avalanche stops at the slope break as observed on Site U1401), but that the avalanche and related submarine debris flow could still trigger far-reaching voluminous failures of the adjacent package of seafloor sediment, even on low gradient slopes.

The likely mechanisms for these large-scale distal seafloor sediment failures (comprising the seismically chaotic landslide deposits) appear to be by decollement propagation from proximal areas of incised volcanic debris avalanche emplacement around the slope break, (Figures 9 and 10), or (in some cases) perhaps by shear traction caused by overrunning debris flow.

The most distal landslide deposits offshore Martinique (U1399) comprises panels of tilted seafloor sediment, which appear otherwise undeformed. A more proximal site (U1400) offshore Martinique displayed panels of tilted and/or microfaulted strata, separated by intervals of homogenized sediment that appear to record multiple layers of intense shear (Figures 5 and 6). The thickness of the homogenized sections may be related to the magnitude of displacement. Thus, it appears that localized and intense shear occurred at multiple horizons at this location, and not just on a single basal surface. A measure of the heterogeneity of these processes is given by the observation that at site U1394 offshore Montserrat, the landslide deposit contains a large flat-lying block of marine strata that appears to be undeformed, although likely displaced (Figure 7). The strength of the sediment package is likely variable from site to site, but the presence of this block suggests it is composed of relatively strong material.

The results of this expedition have important implications for the magnitude of tsunami generation by volcanic island landslides that extend beyond these core sites for the Lesser Antilles. In particular, it is important to recognize that deep and slow landslide deposits comprising mainly of low slope gradient seafloor sediment and involving restricted slip may generate significantly smaller-amplitude tsunamis than landslides with equivalent volumes derived directly from massive failures of the volcanic edifice. Therefore, although the offshore landslides deposits are voluminous and cover large areas, the tsunamis that they could generate will generally be much smaller than more speculative studies have suggested.

IODP Expedition 340 also successfully drilled a series of sites outside the known extent of landslide deposits to capture eruption fallout layers, thereby providing an outstanding data set with which to understand and reconstruct the long-term growth and decay of volcanic islands. The postcruise research now in progress will further illuminate mass-wasting processes over a major volcanic arc, improve the knowledge of volcanic eruptive history that is crucial for hazard and risk assessments, compare the sedimentation processes in the northern and the southern parts of the arc, and provide spatiotemporal correlations of turbidite deposits with deposits resulting from volcanic activity and other causative events.

Acknowledgments
We thank the drillers for their relentless efforts to drill through such difficult volcaniclastic material and all R/V *JOIDES Resolution* staff for their collaboration and efficient work on board. We thank J. McManus for comments on the manuscript. We are very grateful to C. Mével who encouraged and helped us to build our drilling proposal. We thank INSU, NERC, ANR, JSPS, NSF for funding analyses and IPGP for funding postdoc and PhD. We thank the staff of the Montserrat Volcano Observatory, the Martinique and Guadeloupe Volcanological and Seismological Observatory for assistance during the cruise and outreach education activities. Data from the IODP Expedition 340 can be obtained through the expedition's implementing organization USIO (http://iodp.tamu.edu/database).

References

Boudon, G., M. P. Semet, and P. M. Vincent (1984), Flank failure-directed blast eruption at Soufrière, Guadeloupe, French West Indies: A 3,000-yr-old Mt. St. Helens?, *Geology, 12*, 350–353.

Boudon, G., M. P. Semet, and P. M. Vincent (1987), Magma and hydrothermally driven sector collapses: The 3100 and 11500 Y. B.P. eruptions of La Grande Découverte volcano, Guadeloupe, French West Indies, *J. Volcanol. Geotherm. Res.*, *33*, 317–323.

Boudon, G., M. P. Semet, and P. M. Vincent (1992), Major flank collapse at Pitons du Carbet volcano, Martinique: One of the largest similar structures in the lesser Antilles arc, in *29th International Geological Congress*, p. 505, Kyoto, Japan.

Boudon, G., A. Le Friant, B. Villemant, and J.-P. Viodé (2005), Martinique, in *Volcanic Atlas of the Lesser Antilles*, edited by J. M. *Lindsay et al*., pp. 65–102, Seismic Res. Unit, Univ. of the West Indies, Trinidad and Tobago.

Boudon, G., A. Le Friant, J.-C. Komorowski, C. Deplus, and M. P. Semet (2007), Volcano flank instability in the Lesser Antilles Arc: Diversity of scale, processes, and temporal recurrence, *J. Geophys. Res.*, *112*, B08205, doi:10.1029/2006JB004674.

Boudon, G., B. Villemant, A. Le Friant, M. Paterne, and E. Cortijo (2013), Role of large flank-collapse events on magma evolution of volcanoes. Insights from the Lesser Antilles Arc, *J. Volcanol. Geotherm. Res*, *263*, 224–237, doi:10.1016/j.jvolgeores.2013.03.009.

Bouysse, P., and P. Guennoc (1983), Donnes sur la structure de l'arc insulaire des Petites Antilles, entre Sainte Lucie et Anguilla, *Mar. Geol.*, *53*, 131–166.

Bouysse, P., D. Westercamp, and P. Andreieff (1990), The Lesser Antilles Island Arc, in *Proceedings of Ocean Drilling Project, Scientific Results*, edited by J. C. *Moore et al*., pp. 29–44, Ocean Drill. Program, College Station, Tex.

Cassidy, M., J. Trofimovs, M. R. Palmer, P. J. Talling, S. F. L. Watt, S. G. Moreton, and R. N. Taylor (2013), Timing and emplacement dynamics of newly recognised mass flow deposits at ∼8–12 ka offshore Soufrière Hills volcano, Montserrat: How submarine stratigraphy can complement subaerial eruption histories, *J. Volcanol. Geotherm. Res.*, *253*, 1–14.

Cassidy, M., J. Trofimovs, S. F. L.Watt, M. R. Palmer, R. N. Taylor, T. M. Gernon, P. J. Talling, and A. Le Friant (2014), Multi-stage collapse events in the South Soufrière Hills, Montserrat as recorded in marine sediment cores, *Geol. Soc. London*, *39*, 383–397.

Crandell, D. R. (1989), Gigantic debris avalanche of Pleistocene age from ancestral Mount Shasta volcano, California, and debris-avalanche hazard zonation, *U. S. Geol. Surv. Bull.*, *1861*, 32 pp.

Crutchley, G. J., et al. (2013) Insights into the emplacement dynamics of volcanic landslides from highresolution 3D seismic data acquired offshore Montserrat, *Lesser Antilles, Mar. Geol.*, *335*, 1–15, doi:10.1016/j.margeo.2012.10.004.

Delcamp, A., B. van Wyk de Vries, and M. James (2008), The influence of edifice slope and substrata on volcano spreading, *J. Volcanol. Geotherm. Res.*, *177*(4), 925–943.

Deplus, C., A. Le Friant, G. Boudon, J.-C. Komorowski, B. Villemant, C. Harford, J. Ségoufin, and J.-L. Cheminée (2001), Submarine evidence for large-scale debris avalanches in the Lesser Antilles arc, *Earth Planet. Sci. Lett.*, *192*(2), 145–157.

Druitt, T. H., and P. Kokelaar (2002), The eruption of Soufriere Hills Volcano, Montserrat, from 1995 to 1999, *Mem. Geol. Soc. London*, *21*, 639.

Dufresne, A., S. Salinas, and C. Siebe (2010), Substrate deformation associated with the Jocotitlán edifice collapse and debris avalanche deposit, Central México, *J. Volcanol. Geotherm. Res.*, *197*, 133–148.

Feuillet, N., I. Manighetti, P. Tapponnier, and E. Jacques (2002), Arc parallel extension and localization of volcanic complexes in Guadeloupe, Lesser Antilles, *J. Geophys. Res.*, *107*(B12), 2331, doi:10.1029/2001JB000308.

Feuillet, N., et al. (2010), Active faulting induced by slip partitioning in Montserrat and link with volcanic activity: New insights from the 2009 GWADASEIS marine cruise data, *Geophys. Res. Lett.*, *37*, L00E15, doi:10.1029/2010GL042556.

Frey-Martinez, J., J. Cartwright, and D. James (2006), Frontally confined versus frontally emergent submarine landslides: A 3D seismic characterisation, *Mar. Pet. Geol.*, *23*, 585–604.

Gafeira, J., D. Long, R. Scrutton, and D. Evans (2010), 3D seismic evidence of internal structure within Tampen Slide deposits on the North Sea Fan: Are chaotic deposits that chaotic?, *J. Geol. Soc.*, *167*, 605–616.

Garcia, M. O. (1993), Pliocene-Pleistocene volcanic sands from site 842: Products of giants landslides, *Proc. Ocean Drill. Program, Sci. Results*, *136*, 53–63.

Garcia, M. O., S. B. Sherman, G. F. Moore, R. Groll, I. Popova-Goll, J. H. Natland, and G. Acton (2006), Frequent landslides from Koolau Volcano: Results from ODP Hole 1223A, *J. Volcanol. Geotherm. Res.*, *151*, 251–268.

Germa, A., X. Quidelleur, S. Labanieh, P. Lahitte, and C. Chauvel (2010), The eruptive history of Morne Jacob volcano (Martinique Island, French West Indies): Geochronology, geomorphology and geochemistry of the earliest volcanism in the recent Lesser Antilles arc, *J. Volcanol. Geotherm. Res.*, *198*, 297–310.

Glicken, H. (1986), Study of the rockslide avalanche of May 18 1980, Mount St Helens Volcano, PhD thesis, 303 p., Univ. of Calif., Santa Barbara.

Goldstrand, P. M. (1998), Provenance and sedimentologic variations of turbidite and slump deposits at sites 955 and 956, Proc. Ocean Drill. Program, *Sci. Results*, *157*, 343–360.

Harford, C. L., M. S. Pringle, R. S. J. Sparks, and S. R. Young (2002), The volcanic evolution of Montserrat using ^{40}Ar/^{39}Ar geochronology, *Mem. Geol. Soc. London*, *21*, 93–113.

Holcomb, R., and R. Searle (1991), Large landslides from oceanic volcanoes, *Mar. Geotechnol.*, *10*, 19–32.

Hunt, J. E., R. B. Wynn, D. G. Masson, P. J. Talling, and D. A. H. Teagle (2011), Sedimentological and geochemical evidence for multistage failure of volcanic landslides: A case study from Icod landslide on north Tenerife, Canary Islands, *Geochem. Geophys. Geosyst.*, *12*, Q12007, doi:10.1029/2011GC003740.

Ida, Y., and B. Voight (Eds.) (1995), Models of magmatic processes and volcanic eruptions. *J. Volcanol. Geotherm. Res.*, *66*, 426.

Iverson, R. M. (1997), The physics of debris flows, *Rev. Geophys.*, *35*, 245–296.

Jutzeler, M., J. D. L. White, P. J. Talling, M. McCanta, S. Morgan, A. Le Friant, and O. Ishizuka (2014), Coring disturbances in IODP piston cores with implications for offshore record of volcanic events and the Missoula megafloods, *Geochem. Geophys. Geosyst.*, *15*, 3572–3590, doi:10.1002/2014GC005447.

Karstens, J., G. J. Crutchley, C. Berndt, P. J. Talling, S. F. L. Watt, J. Trofimovs, V. Hühnerbach, A. Le Friant, and E. Lebas (2013), Insights into pyroclastic flow emplacement from high-resolution 3D seismic data offshore Montserrat, Lesser Antilles, *J. Volcanol. Geotherm. Res.*, *257*, 1–11.

Komorowski, J. C., G. Boudon, M. Semet, F. Beauducel, C. Anténor-Habazac, S. Bazin, and G. Hammouya (2005), Guadeloupe, in *Volcanic Hazard Atlas of the Lesser Antilles, published by University of the West Indies*, edited by J. *Lindsay et al*., pp. 65–102, Seismic Res. Unit, Trinidad and Tobago.

Krastel, S., H. U. Schmincke, C. L. Jacobs, R. Rihm, T. M. Le Bas, and B. Alibés (2001), Submarine landslides around the Canary Islands, *J. Geophys. Res.*, *106*, 3977–3997.

Labazuy, P. (1996), Recurrent landslides events on the submarine flank of Piton de la Fournaise volcano (Reunion Island), in *Volcano Instability on the Earth and Other Planets, Geol. Soc. Spec. Publ*., vol. 110, edited by W. J. McGuire, A. P. Jones and J. Neuberg, pp. 295–306, London, U. K., doi: 10.1144/GSL.SP.1996.110.01.23.

Lafuerza S., A. Le Friant, M. Manga, G. Boudon, B. Villemant, N. Stroncik, B. Voight, M. Hornbach, O. Ishizuka and the Expedition 340 Scientific Party (2014), Geomechanical characterizations of submarine volcano flank sediments, Martinique, Lesse Antilles Arc, in Sumarine Mass Movements and Consequences, Adv. Nat. Technol. Hazards Res., edited by S. Krastel et al., p. 37, Springer, Switzerland, doi: 10.1007/978-3-319-00972-8_7.

Lebas, E., A. Le Friant, G. Boudon, S. Watt, P. Talling, N. Feuillet, C. Deplus, C. Berndt, and M. Vardy (2011), Multiple widespread landslides during the long-term evolution of a volcanic island: Insights from high-resolution seismic data, Montserrat Lesser Antilles. *Geochem. Geophys. Geosyst.*, *12*, Q05006, doi:10.1029/2010GC003451.

Le Friant, A., G. Boudon, J-C. Komorowski, and C. Deplus (2002), L'île de la Dominique, à l'origine des avalanches de débris les plus volumineuses de l'arc des Petites Antilles, *C. R. Geosci.*, *334* (4), 235–243.

Le Friant, A., G. Boudon, C. Deplus, and B. Villemant (2003a), Large scale flank collapse events during the activity of Montagne Pelée, Martinique, Lesser Antilles, *J. Geophys. Res.*, *108*(B1), 2055, doi:10.1029/2001JB001624.

Le Friant, A., P. Heinrich, C. Deplus, and G. Boudon (2003b), Numerical simulation of the last flank collapse event of Montagne Pelée, Martinique, Lesser Antilles, *Geophys. Res. Lett*. *30*(2), 1034, doi:10.1029/2002GL015903.

Le Friant, A., C. Harford, C. Deplus, G. Boudon, S. Sparks, R. Herd, and J.-C. Komorowski (2004), Geomorphological evolution of Montserrat (West Indies): Importance of flank collapse and erosional processes, *Geol. Soc. London*, *161*, 147–160.

Le Friant, A., E. J. Lock, M. B. Hart, M. J. Leng, C. W. Smart, R. S. J. Sparks, G. Boudon, C. Deplus, and J. C. Komorowski (2008), Late Pleistocene tephrochronology of marine sediments adjacent to Montserrat, Lesser Antilles volcanic arc, *J. Geol. Soc. London*, *165*, 279–289.

Le Friant, A., G. Boudon, A. Arnulf, and R. Robertson (2009), Debris avalanche deposits offshore St Vincent (West Indies): Impact of flank-collapse events on the morphological evolution of the island, *J. Volcanol. Geotherm. Res*, *179*, 1–10.

Le Friant, A., et al. (2010), Eruption of Soufrière Hills (1995–2009) from an offshore perspective: Insights from repeated swath bathymetry surveys, *Geophys. Res. Lett.*, *37*, L11307, doi:10.1029/2010GL043580.

Le Friant, A., E. Lebas, V. Clément, G. Boudon, C. Deplus, B. de Voogd, and P. Bachèlery (2011), A new model for the evolution of la Réunion volcanic complex from complete geophysical surveys, *Geophys. Res. Lett.*, *38*, L09312, doi:10.1029/2011GL047489.

Le Friant, A., O. Ishizuka, N. A. Stroncik, and the Expedition 340 Scientists (2013), *Proceedings of Integrated Ocean Drilling Program, 340*, Integrated Ocean Drill. Program Manage. Int. Inc., Tokyo, doi:10.2204/iodp.proc.340.2013.

Lindsay, J. M., R. E. A. Robertson, J. B. Shepherd, and S. Ali (Eds.) (2005), *Volcanic Hazards Atlas of the Lesser Antilles*. Seismic Res. Unit, Univ. of the West Indies, Trinidad and Tobago.

Lipman, P. W., W. R. Normark, J. G. Moore, J. B. Wilson, and E. Gutmacher (1988), The giant submarine Alika debris slide, Mauna Loa, Hawaii, *J. Geophys. Res.*, *93*, 4279–4299.

Løvholt, R., G. Pedersen, and G. Gisler (2008), Oceanic propagation of a potential tsunami from the La Palma Island, *J. Geophys. Res.*, *113*, C09026, doi:10.1029/2007JC004603.

MacDonald, R., C. J. Hawkesworth, and E. Heath (2000), The Lesser Antilles volcano chain; a study in arc magmatism, *Earth Sci. Rev.*, *49*, 1–76.

Manga M., et al. (2012), Heat flow in the Lesser Antilles island arc and adjacent back arc Grenada basin, *Geochem. Geophys. Geosyst.*, *13*, Q08007, doi:10.1029/2012GC004260.

Martin-Kaye, P. H. A. (1969), A summary of the geology of the Lesser Antilles, *Overseas Geol. Miner. Res.*, *10*(2), 172–206.

Masson, D. G., A. B. Watts, M. J. R. Gee, R. Urgeles, N. C. Mitchell, T. P. Le Bas, and M. Canals (2002), Slope failures on the flanks of the western Canary Islands, *Earth Sci. Rev.*, *57*, 1–35.

Masson, D. G., C. B. Harbitz, R. B. Wynn, G. Pedersen, and F. Løvholt (2006), Submarine landslides: Processes, triggers and hazard prediction, *Philos. Trans. R. Soc. A*, *364*, 2009–2039.

Mattioli, G. S., et al. (2007), Unique and remarkable dilatometer measurements of pyroclastic flow-generated tsunamis, *Geology*, *35*, 25–28.

McGuire, W. J. (1996), Volcano instability: a review of contemporary themes, in *Volcano Instability on the Earth and Other Planets, Geol. Soc. Spec. Publ*., vol. 110, edited by W. J. McGuire et al., pp. 1–23, doi:10.1144/GSL.SP.1996.110.01.01.

Montanaro, C., and J. Beget (2011), Volcano collapse along the Aleutian Ridge (western Aleutian Arc), *Nat. Hazards Earth Syst. Sci.*, *11*, 715–730, doi:10.5194/nhess-11-715-2011.

Moore, J. G., and D. A. Clague (2002), Mapping the Nuuanu and Wailau landslides in Hawaii, in *Hawaiian Volcanoes: Deep underwater Perspectives*, edited by E. Takahashi et al., pp. 223–244, AGU, Washington, D. C., doi:10.1029/GM128p0223.

Moore, J. G., D. A. Clague, R. T. Holcomb, P. W. Lipman, W. R. Normark, and M. E. Torresan (1989), Prodigious submarine landslides on the Hawaiian ridge, *J. Geophys. Res.*, *94*, 17,465–17,484.

Oehler, J. F., J. F. Lenat, and P. Labazuy (2008), Growth and collapse of the Reunion Island volcanoes, *Bull. Volcanol.*, *70*, 717–742, doi:10.1007/s00445-007-0163-0.

Paterne, M. (1985), Reconstruction de l'activité explosive des volcans de l'Italie du Sud par téphrochronologie marine, PhD thesis, 144 pp., Univ. of Paris, Paris.

Paterne, M., F. Guichard, G. Duplessy, G. Siani, R. Sulpizio, and J. Labeyrie (2008), A 90000–200000 yrs marine tephra record of Italian volcanic activity in the central Mediterranean Sea, *J. Volcanol. Geotherm. Res.*, *177*, 187–196, doi:10.1016/j.jvolgeores.2007.11.028.

Picard, M., J.-L. Schneider, and G. Boudon (2006), Contrasting sedimentary processes along a convergent margin: The Lesser Antilles arc system, *Geo Mar. Lett.*, *26*(6), 397–410.

Pinel, V., and F. Albino (2013), Consequences of volcano sector collapse on magmatic storage zones: Insights from numerical modeling, *J. Volcanol. Geotherm. Res.*, *252*, 29–37.

Pinel, V., and C. Jaupart (2000), The effect of edifice load on magma ascent beneath a volcano, *Philos. Trans. R. Soc. London A*, *358*, 1515–1532.

Reid, R. P., S. N. Carey, and D. R. Ross (1996), Late Quaternary sedimentation in the Lesser Antilles island arc, *Geol. Soc. Am. Bull.*, *108*(1), 78–100.

Samper, A., X. Quidelleur, G. Boudon, A. Le Friant, and J.-C. Komorowski (2008), Radiometric dating of three large volume flank-collapses in the Lesser Antilles Arc, *J. Volcanol. Geotherm. Res.*, *176*, 485–492, doi:10.1016/j.jvolgeores.2008.02.028.

Schmincke, H.-U., and M. Sumita (1998), Volcanic evolution of Gran Canaria reconstructed from apron sediments: Synthesis of vicap project drilling, *Proc. Ocean Drill. Program Sci. Results*, *157*, 443–469.

Schneider, J.-L., et al. (1997), Du volcan au sediment: La dynamique du talus volcanoclastique sous-marin de Gran Canaria, Canaries (Atlantique oriental, Leg ODP 157), *C. R. Acad. Sci., Ser. IIa Sci. Terre Planetes*, *324*, 891–898.

Siebe, C., J.-C. Komorowski, and M. F. Sheridan (1992), The tectonically induced avalanche deposit at Jocotitlán volcano, central Mexico: Unusual morphology, stratigraphical relations, and possible mode of emplacement, *Bull. Volcanol.*, *54*, 573–589.

Siebert, L. (2002), Landslides resulting from structural failures in volcanoes, in *Catastrophic Landslides: Effects, Occurrence, and Mechanisms*, edited by S. G. Evans, and J. V. DeGraff, *Rev. Eng. Geol*., vol. XV, p. 209–235, Geol. Soc. of Am., Boulder, Colo.

Sigurdsson, H., R. S. J. Sparks, S. Carey, and T. C. Huang (1980), Volcanogenic sedimentation in the Lesser Antilles Arc, *J. Geol.*, *88*, 523–540.

Silver, E., S. Day, S. Ward, G. Hoffmann, P. Llanes, N. Driscoll, B. Appelgate and S. Saunders (2009), Volcano collapse and tsunami generation in the Bismark Volcanic Arc, Papua New Guinea, *J. Volcanol. Geotherm. Res.*, *186*, 210–222, doi:10.1016/j.jvolgeores.2009.06.013.

Slingerland, R., and B. Voight (1979), Occurrence and predictive models for slide-generated water waves, in *Rockslides and Avalanches*, vol. 2, edited by B. Voight, pp. 317–400, Elsevier, Amsterdam.

Smith, A. L., M. J. Roobol, J. H. Schellekens, and G. S. Mattioli (2007), Prehistoric stratigraphy of the Soufrière Hills–South Soufrière Hills volcanic complex, Montserrat, West Indies, *J. Geol.*, *115*, 115–127, doi:10.1086/509271.

Sparks, R. S. J., J. Barclay, E. S. Calder, R. A. Herd, J. C. Komorowski, G. E. Norton, L. Ritchie, B. Voight, and A. W. Woods (2002), Generation of a debris avalanche and violent pyroclastic density current: The Boxing Day eruption of 26 December 1997 at the Soufriere Hills Volcano, Montserrat, in The eruption of Soufriere Hills Volcano, Montserrat, From 1995 to 1999, Geol. Soc. Mem., vol. 21, edited by T. H. Druitt, and B. P. Kokelaar, pp. 409–434, *Geol. Soc. Mem.*, London, U. K.

Talling, P. J., G. Malgesini, E. J. Summer, L. A. Amy, F. Felletti, G. Blackboum, C. Nutt, C. Wilcox, I. C. Harding, and S. Akbari (2012), Planform geometry, stacking pattern, and extrabasinal origin of low strength and intermediate strength cohesive debris flow deposits in the Marnoso-arenacea Formation, Italy, *Geosphere*, *8*(6), 1207–1230, doi:10.1130/GES00734.1.

Trofimovs, J., et al. (2006), What happens when pyroclastic flows enter the ocean?, *Geology*, *34*, 549–552.
Trofimovs, J., R. S. J. Sparks, and P. J. Talling (2008), Anatomy of a submarine pyroclastic flow and associated turbidity current: July 2003 dome collapse, Soufrière Hills volcano, Montserrat, West Indies, *Sedimentology*, *55*, 617–634.
Trofimovs, J., et al. (2010), Evidence for carbonate platform failure during rapid sea-level rise; ca 14 000 year old bioclastic flow deposits in the Lesser Antilles, *Sedimentology*, *57*(3), 735–759.
Trofimovs, J., et al. (2012), Sumarine pyroclastic deposits formed during the 20th May 2006 dome collapse of the Soufrière Hills volcano, Montserrat, *Bull. Volcanol.*, *74*, 391–405, doi:10.1007/s00445-011-0533-5.
Trofimovs, J., et al. (2013), Timing, origin and emplacement dynamics of mass flows offshore of SE Montserrat in the last 110 ka: Implications for landslide and tsunami hazards, eruption history, and volcanic island evolution, *Geochem. Geophys. Geosyst.*, *14*, 385–406, doi: 10.1002/ggge.20052.
Urgeles, R., M. Canals, J. Baraza, B. Alonso, and D. Masson (1997), The most recent megalandslides of the Canary Islands: El Golfo debris avalanche and Canary debris flow, west El Hierro Island, *J. Geophys. Res.*, *102*, 20,305–20,323.
Viesca, R. C., and J. R. Rice (2012), Nucleation of slip-weakening rupture instability in landslides by localized increase of pore pressure, *J. Geophys. Res.*, *117*, B03104, doi:10.1029/2011JB008866.
Vincent, P. M., J.-L. Bourdier, and G. Boudon (1989), The primitive volcano of Mount Pelée: Its construction and partial destruction by flank collapse, *J. Volcanol. Geotherm. Res.*, *38*, 1–15.
Voight, B. (1981), Time scale for the first moments of the May 18 eruption, *U.S. Geol. Surv. Prof. Pap.*, *1250*, 69–86.
Voight, B. (2000), Structural stability of andesite volcanoes and lava domes, *Philos. Trans. R. Soc. London A*, *358*, 1663–1703.
Voight, B., and D. Elsworth (1997), Failure of volcano slopes, *Geotechnique*, *47*, 1–31.
Voight, B., R. J. Janda, H. Glicken and P. M. Douglass (1981), Catastrophic rockslide avalanche of May 18, *U.S. Geol. Surv. Prof. Pap.*, *1250*, 347–378.
Voight, B., et al. (2002), The 26 December (Boxing Day) 1997 sector collapse and debris avalanche at Soufrière Hills Volcano, Montserrat, in *The Eruption of Soufriere Hills Volcano, Montserrat, From 1995 to 1999*, Geological Society, London, Memoirs 2002, vol. 21, edited by T. H. Druitt and B. P. Kokelaar, pp. 363–407, doi:10.1144/GSL.MEM.2002.021.01.17.
Voight, B., A. Le Friant, G. Boudon, C. Deplus, J. C. Komorowski, E. Lebas, R. S. J. Sparks, P. Talling, and J. Trofimovs (2012), Undrained sediment loading key to long-runout submarine mass movements: Evidence from the Caribbean Volcanic Arc, in *Submarine Mass Movements and Their Consequences, Adv. Nat. Technol. Hazards Res.*, vol. 31, edited by Y. Yamada, et al., pp. 417–428, doi:10.1007/978-94-007–62-3–37.
Wadge, G. (1984), Comparison of volcanic production rates and subduction rates in the Lesser Antilles and Central America, *Geology*, *12*, 555–558.
Wadge, G. (1986), The dykes and structural setting of the volcanic front in the Lesser Antilles island Arc, *Bull. Volcanol.*, *48*, 349–372.
Wadge, G., B. Voight, R. S. J. Sparks, P. D. Cole, S. C. Loughlin, and R. E. A. Robertson (2014), Chapter 1. An overview of the eruption of Soufrière Hills Volcano, Montserrat from 2000 to 2010, in *The Eruption of Soufrière Hills Volcano, Montserrat From 2000 to 2010, Geol. Soc. Mem. 39*, edited by G. Wadge, , R. E. A. Robertson, and B. Voight, pp. 1–39, *Geol. Soc. Mem.*, London, U. K., doi:10.1144/M39.1.
Wall-Palmer, D., et al. (2014), Late Pleistocene stratigraphy of IODP U1396 and compiled chronology offshore of south and south west Montserrat, Lesser Antilles, *Geochem. Geophys. Geosyst.*, *15*, 3000–3020, doi:10.1002/2014GC005402.
Ward, S. N. (2001), Landslide tsunami, *J. Geophys. Res.*, *106*, 11,201–11,215.
Ward, S. N. and S. J. Day (2001), Cumbre Vieja volcano–Potential collapse and tsunami at La Palma, Canary Islands, *Geophys. Res. Lett.*, *28*, 3397–3400.
Watt, S. F. L., et al. (2012a), Combination of volcanic-flank and seafloor sediment failure offshore Montserrat, and their implications for tsunami generation, *Earth Planet. Sci. Lett.*, *319*(2), 228–240, doi:10.1016/j.epsl.2011.11.032.
Watt, S. F. L., et al. (2012b), Widespread and progressive seafloor-sediment failure following volcanic debris avalanche emplacement: Landslide dynamics and timing offshore Montserrat, Lesser Antilles, *Mar. Geol.*, *323*, 69–94, doi:10.1016/j.margeo.2012.08.002.
Watt, S. F. L., P. J. Talling, and J. E. Hunt (2014), New insights into the emplacement dynamics of volcanic-island landslides, *Oceanography*, *27*, 46–57.
Watts, A. B., and D. G. Masson (1995), A giant landslide on the north flank of Tenerife, Canary Islands, *J. Geophys. Res.*, *100*, 24,487–24,498.
Watts, P., S. T. Grilli, D. R. Tappin, and G. J. Fryer (2005), Tsunami generation by submarine mass failure. II: Predictive equations and case studies. *J. Waterw. Port Coastal Ocean Eng.*, *131*, 298–310.
Westercamp, D., and H. Traineau (1983), Carte géologique au 1/20 000 de la Montagne Pelée, avec notice explicative, *BRGM, Orléans, France*.